types of mutations in hereditary NBL[18–22]. More recently, Passoni *et al.* described NBL patients with high levels of ALK expression without *ALK* gene mutations. They showed that regardless of mutation status, high ALK levels were strongly correlated with poor prognosis[23]. This correlation between high ALK levels and unfavorable prognosis was also confirmed by some other investigators[24–26]. Moreover, Di Paolo *et al.* demonstrated that RNA interference (RNAi)-based knockdown of ALK, regardless of its genetic status, showed reduced proliferation and increased apoptosis in NBL cells and inhibited NBL tumor growth as well as prolonged survival *in vivo*[27].

In the present study, we found that ALK directly mediates MYCN-induced oncogenic properties. The promoter region of *ALK* gene contains a non-canonical E-box located upstream of the transcription initiation site, and MYC proteins bind onto the promoter region and regulate its transcription. Wild-type ALK functions as a modulator of proliferation as well as cell migration and invasion. In addition, those biological activities and tumor growth in xenograft model derived from NBL cell lines with *MYCN* amplification were inhibited by targeting wild-type ALK with TAE-684, suggesting that highly expressed ALK in *MYCN* amplified cells could be inhibited by ALK inhibitor in the same manner as mutated or amplified *ALK*. These findings may be beneficial to the understanding of the molecular mechanism of wild-type ALK function, and contribute to the development of a possible therapeutic strategy for ALK-expressing NBLs.

Results

***ALK* mRNA expression is associated with *MYCN* amplification and expression in neuroblastomas.** The expression of *MYCN* and *ALK* mRNA was measured by quantitative real-time PCR (qRT-PCR) for cDNA samples obtained from NBL clinical tissues. *MYCN* expression was significantly higher in tumors with *MYCN* amplification than *MYCN*-non-amplified tumors ($P < 0.001$; Figure 1a). In this subset of NBLs with *MYCN* amplification, mRNA expression of *ALK* was significantly higher as compared with *MYCN*-non-amplified tumors ($P < 0.01$; Figure 1a). High expression of *ALK* was also observed in NBLs at stages 3, 4 and 4S (Figure 1b), suggesting that *ALK* might contribute to an aggressiveness and metastasis of NBL.

Both MYCN and c-Myc regulates *ALK* expression. In a *MYCN* transgenic mice model, the expression of the human *MYCN* oncogene was targeted to neural crest cells with the use of a tyrosine hydroxylase promoter[12]. This promoter is active in migrating cells of the neural crest early in the development of sympathetic ganglia and the adrenal medulla from which NBLs often arise[28]. Expression of both human *MYCN* and endogenous *Alk* mRNA was induced in superior mesenteric ganglion (SMG) tissues of 2-week-old *MYCN*-hemizygous mice (Figure 1c), which continued in adrenal tumor tissues until the mice were at least 11 weeks old. Consistent with the transgenic mice data, overexpression of *MYCN* or *c-Myc* in NBL (wild-type *ALK* cell line; NBL-S and NLF, and mutated *ALK* cell line; SH-SY5Y) and non-NBL (U2OS and HeLa) cells induced *ALK* expression in dose- and time-dependent manners at the mRNA (Figures 2a–c and Supplementary Figure S1A) and protein (Supplementary Figures S1B and C) levels. Next, we performed siRNA-mediated knockdown of *MYCN* experiment in SK-N-AS cells as described previously[29], and found that *MYCN* knockdown decreased expression of *ALK* (Figure 2d). To confirm a possible relationship between *MYCN* and *ALK*, we employed *MYCN*-inducible neuroblastoma cells (Tet21/N) derived from a parental neuroblastoma cell line, SHEP[8]. The Tet21/N cells constitutively expressed *MYCN* in the absence of tetracycline (Tc), whereas the addition of Tc to the culture decreased *MYCN* expression levels. At the indicated time points after Tc depletion, total RNA was prepared and subjected to RT–PCR. As shown in Figure 2e, Tc deprivation led to an induction of *MYCN* in association with a significant increase in the expression levels of *ALK*. In contrast, addition of Tc significantly reduced the expression levels of *MYCN* with a concomitant decrease in *ALK* expression levels (Figure 2e), suggesting that *ALK* might be a direct transcriptional target of MYCN.

***ALK* is a direct transcriptional target of MYCN and c-Myc.** To identify a possible promoter region of *ALK* gene, we generated luciferase reporter constructs containing −2056 bp to +30 bp fragments of *ALK* gene. We performed promoter study using NBL (mutated *ALK* cell line; SH-SY5Y and wild-type *ALK* cell line; SK-N-AS) and non-NBL (U2OS and HeLa) cells, which showed co-related regulation of *ALK* gene with MYCN or c-MYC expression (Figures 2b–d and Supplementary Figure S1A). An increase in luciferase activity was observed in cells transfected with pGL4.17 *ALK* (−2056 bp) compared with empty pGL4.17-basic vector (Figure 3a and Supplementary Figure S2A). The luciferase activity with pGL4.17 *ALK* (−2056 bp) was enhanced by co-expression of increasing amounts of *MYCN* or *c-Myc* expression vector (Figure 3b and Supplementary Figure S2B).

Next, we performed ChIP assays with anti-MYCN and anti-c-Myc antibodies to determine whether they could directly bind to the *ALK* promoter. As shown in Figure 3c, MYCN was recruited onto the *ALK* promoter region. Endogenous MYCN was recruited onto the same region in TNB1 cells (*MYCN* amplification and high expression of *ALK*, Supplementary Figure S7A) but not in RISA cells (*MYCN*-non-amplified and low *ALK* expression). Moreover, in non-NBL cell lines, the recruitment of endogenous c-Myc was more obvious in A875 cells (high *ALK* expression, Supplementary Figure S7B) than HeLa cells (low *ALK* expression) (Figure 3c). Since the region to which MYC proteins were recruited contains two possible E-boxes (E-box1 and E-box2), E-box deletions were introduced in the luciferase reporter construct (−350 bp). Deletion of the E-box1 and/or E-box2 resulted in a significant reduction of *ALK* gene promoter activity in SK-N-AS (Figure 3d) and HeLa cells (Supplementary Figure S2C).

ALK shows oncogenic potential in NBL cells. Consistent with previous reports[23,30], our results also showed that ectopic expression of wild-type or mutated (F1174L) ALK induced the phosphorylation of both ALK and an ALK-associated signaling molecule, AKT (Supplementary Figure S4A). The siRNA-mediated knockdown of endogenous ALK resulted in reduced phosphorylation of AKT in NBL cells harboring a wild-type allele (Supplementary Figure S4B). Next, we investigated cell growth study using NBL cells (SK-N-DZ, SK-N-AS and NBL-S), which showed activation of the downstream signaling molecule AKT by ALK overexpression (Supplementary Figure S4A). We also performed siRNA mediated knockdown of *ALK* experiment in *MYCN* amplified NLF cells. Figure 4a and 4b shows that overexpression of *ALK* enhanced cell proliferation, whereas siRNA-mediated knockdown of *ALK* was correlated with an inhibition of proliferation of NBL cells. Colony formation assays also revealed that the number and size of *ALK*-expressing viable clones were higher than those of vector control cells (Figures 4c and 4d).

To examine whether ALK contributes to metastatic activity of NBL cells, we performed wound healing assays in *MYCN*-non-amplified NBL (mutated *ALK* cell line; SH-SY5Y and wild-type *ALK* cell line; SK-N-AS) and low *ALK* expressing non-NBL (HeLa) cells, and found that ALK expression enhanced cell migration (Supplementary Figure S5). Consistent with these results, Boyden chamber migration and invasion assays also showed a significant increase in the number of migrated and invaded cells arising from ALK-expressing cells compared with the vector control cells (Figure 5a and Supplementary Figure S6A). This study we performed using *MYCN*-non-amplified cell line SK-N-AS, as shown downstream signaling molecule AKT was activated upon ALK overexpression (Supplementary Figure S4A), and low *ALK* expressing non-NBL cell line HeLa.

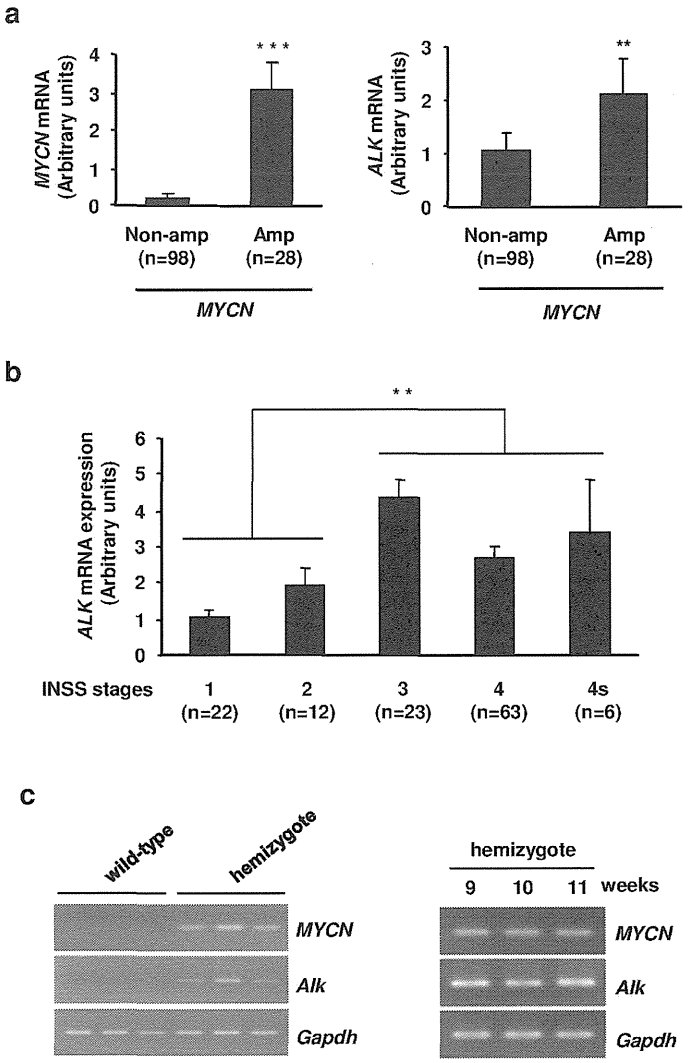

Figure 1 | Endogenous *ALK* expression is correlated with *MYCN* expression levels. (a) *ALK* expression in NBL clinical samples. The expression levels of *MYCN* (left) and *ALK* (right) mRNA in subsets of *MYCN*-non-amplified and amplified NBL clinical samples. (b) *ALK* mRNA in different stages of NBL (INSS stages). (c) High expression of *MYCN* and *Alk* mRNA in *MYCN*-transgenic mice. *MYCN* and *Alk* expression were investigated by RT-PCR in SMG tissues of 2-week-old wild-type and *MYCN*-hemizygous mice (left) and in adrenal gland tumor tissues of *MYCN*-hemizygous mice at 9, 10 and 11 weeks old (right).

Migration and invasion of NBL cells were significantly suppressed by knockdown of *ALK* expression (Figure 5b and Supplementary Figure S6B). For knockdown of ALK experiment, we used *MYCN*-non-amplified NBL-S cells, which have a high expression of MYCN protein and invasive potency as described previously[10], and phosphorylation of the downstream molecule AKT was reduced with ALK knockdown (Supplementary Figure S4B). We also performed knockdown of ALK study in *MYCN* amplified cell line SK-N-DZ. Both cell lines have a wild-type *ALK* allele.

ALK mediates MYCN-induced oncogenesis. We next tested the effect of growth inhibitory stimulus such as retinoic acid (RA) on the proliferative and colony-forming ability of cells expressing wild-type or F1174L-mutant *ALK*. RA is a well known MYCN suppressor, and the addition of RA to proliferating NBL cells halts their division and leads to either differentiation or apoptosis[31–33]. We analyzed RA treatment experiment using *MYCN* amplified NBL cells (GOTO), which have a wild-type *ALK* allele and showed sensitivity to RA as previously described[33]. Figures 6a and b showed that after treatment with RA, the proliferation as well as the number and size of colony of NBL cells were significantly suppressed. As expected, *MYCN* expression was decreased after RA treatment, and *ALK* expression was also downregulated (Figure 6c). However, both wild-type and F1174L mutated *ALK*-overexpressing cells had a higher number of live clones compared with the control cells following treatment with RA, suggesting that the prior *ALK* expression partially prevented the effect of RA on cell proliferation.

We also examined the effect of MYCN-induced cell migration in the presence or absence of *ALK* expression. This study we performed using NBL-S cells, which showed upregulation of endogenous ALK with MYCN overexpression (Figure 2a and Supplementary Figure S1B). Consistent with previous reports[10,11], *MYCN* expression enhanced cell migration. As expected, the migration was suppressed by siRNA-mediated knockdown of *ALK* in NBL cells (Figure 6d), suggesting that MYCN function in cell migration is at least partly regulated by *ALK* expression.

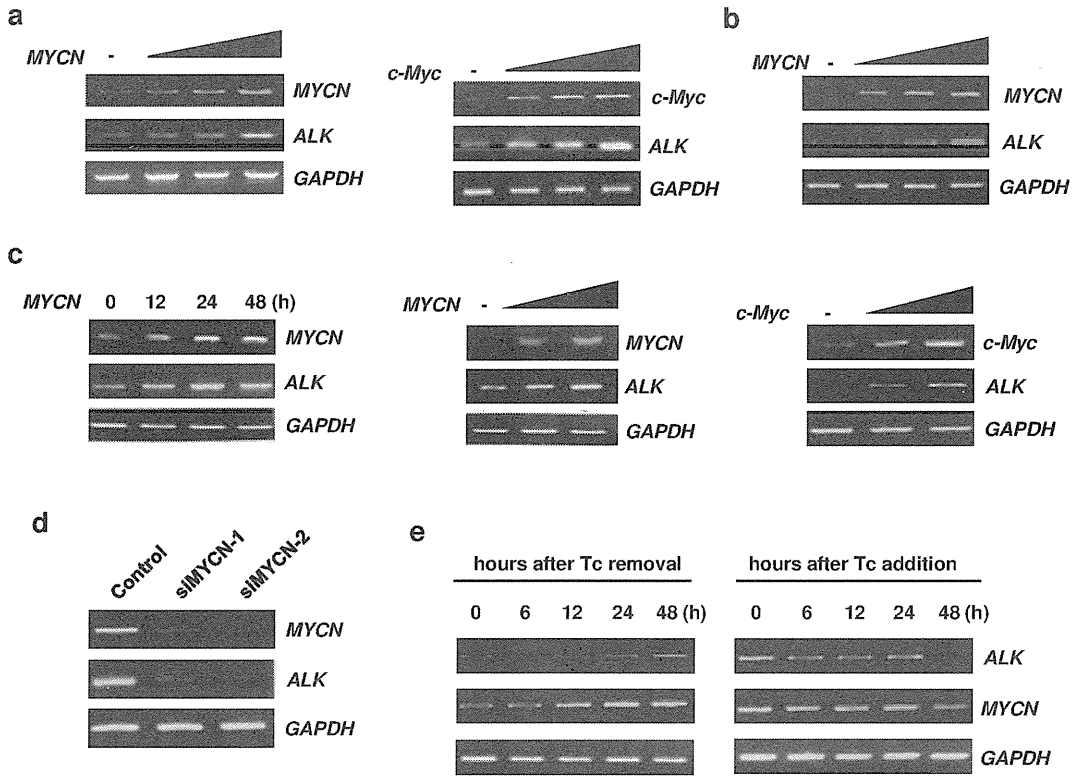

Figure 2 | MYC proteins regulate the expression of *ALK*. (a) NBL-S cells were transfected with different amounts of *MYCN* or *c-Myc* expression vector. (b) SH-SY5Y (F1174L *ALK* mutation) cells were transfected with *MYCN* expression vector as (a). (c) U2OS cells were transfected with *MYCN* or *c-Myc* expression vector, and the expression of *ALK* mRNA was examined in a time- (left) or dose- (middle and right) dependent manner. At the indicated time points (for time-dependent) or at 24 h (for dose-dependent) after transfection, the expression of *ALK*, *MYCN* or *c-MYC* was checked by RT-PCR. (d) siRNA-mediated knockdown of *MYCN* downregulated *ALK* expression. SK-N-AS cells were transfected with control siRNA or siRNA targeting *MYCN* (si*MYCN*-1 and -2). Seventy-two hours after transfection, total RNA was prepared and processed for RT-PCR. (e) Induction of *ALK* in *MYCN*-inducible SHEP Tet21/N cells (F1174L *ALK* mutation). RT-PCR of *ALK* and *MYCN* expression was performed after the removal (left) or addition (right) of tetracycline (Tc, 100 ng/ml) at the indicated time intervals.

ALK inhibitors suppressed NBL cell growth, migration and invasion, and inhibited tumor growth in xenograft model. Finally, we analyzed the effect of ALK inhibition on NBL cell proliferation, migration and invasion. Cell proliferation of NBL cells with *MYCN* amplification (SK-N-DZ, NLF and GOTO) were effectively inhibited by TAE-684 compared to *MYCN*-non-amplified cells (SK-N-AS and RISA) (Figure 7a). The IC_{50} values of SK-N-DZ, NLF, GOTO, RISA and SK-N-AS cells were 75.6 nM, 95.5 nM, 132.7 nM, 349.0 nM and 894.7 nM, respectively. Consistence with these results, efficient suppression of cell migration and invasion were observed in *MYCN* amplified NBL cells (SK-N-DZ and NLF) after TAE-684 treatment, whereas no significant suppression was detected in *MYCN*-non-amplified SK-N-AS cells (Figure 7b). Similar results in cell growth and migration assays using NBL cells with *MYCN* amplification were obtained by two selective ALK inhibitors, crizotinib and CH5424802 (Supplementary Figure S8). In addition, TAE-684 treatment significantly suppressed tumor growth of xenograft generated from *MYCN* amplified NBL cells (SK-N-DZ and NLF) (Figure 7c).

Discussion

MYCN amplification occurs in approximately 25% of primary NBLs and is one of the most reliable prognostic factors identified to date[1,5–7]. It is significantly associated with advanced disease stages, rapid tumor progression and poor prognosis. However, the molecular mechanisms how MYCN induces aggressive NBL have not yet been fully elucidated. Our present findings clearly provided the evidence that MYCN-mediated *ALK* induction promotes cell proliferation, migration and invasion.

To our knowledge, this is the first report showing a direct role of MYCN in the transcriptional regulation of *ALK* in NBL. Consistent with the evidence that *ALK* expression was significantly correlated with *MYCN* amplification in primary NBLs, overexpression of *MYCN* induced promoter activity of the *ALK* gene, leading to a high level of *ALK* expression in NBL cells. The induction of *ALK* expression was also observed in non-NBL cells, suggesting that the transcription of *ALK* gene is generally regulated by MYCN. Moreover, in agreement with the previous results showing that c-Myc recognizes and binds to the E-box in the same manner as MYCN[14,15,34], *ALK* expression was also transcriptionally regulated by c-Myc in non-NBL cells. Taking this into account, *ALK* is a direct target gene of MYC proteins. Our data are also informative to explain why *ALK* expression is high in *MYCN* transgenic mice. High levels of *ALK* expression were observed in 2-week-old *MYCN*-hemizygous mice, indicating that a spontaneously arising NBL expresses *ALK* in the early stage of tumor development driven by MYCN. Recently, PHOX2b has been reported as a transcription factor targeting *ALK*[35]. While the researchers identified transcriptional activity in the promoter construct of *ALK* gene from −672 to +384 bp, we observed comparable basal promoter activity in the −350 to +30 bp promoter region that

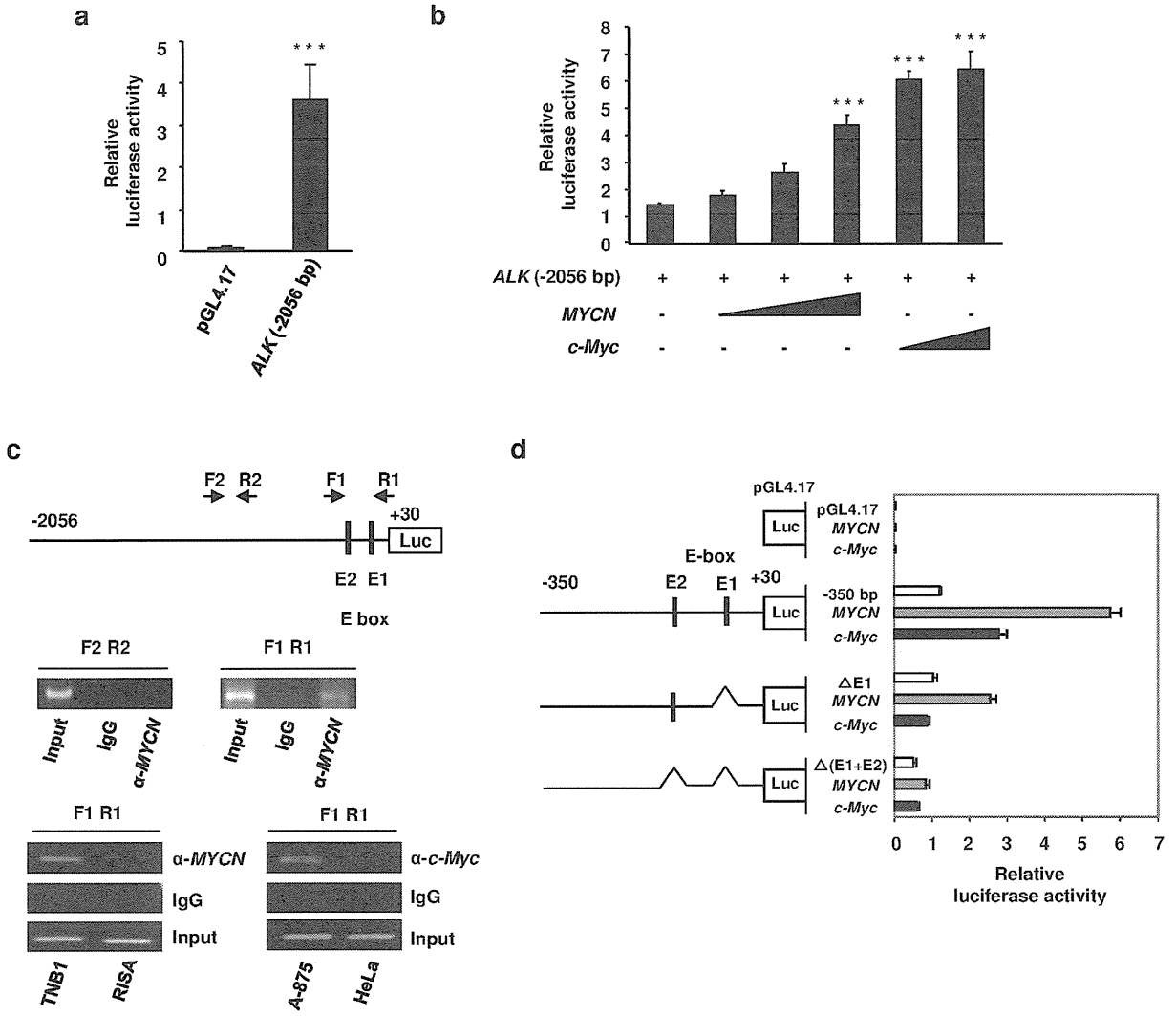

Figure 3 | Transcription of *ALK* is directly regulated by MYC proteins. (a) SH-SY5Y cells were transfected with *ALK* luciferase reporter construct (−2056 bp) or empty vector and subjected to luciferase reporter assays. (b) Overexpression of both *MYCN* and *c-Myc* enhanced the basal promoter activity of *ALK*. SH-SY5Y cells were co-transfected with *ALK* (−2056 bp) and increasing amounts of *MYCN* or *c-Myc* expression vector. Luciferase assays were then performed to measure the promoter activity. (c) Both MYCN and c-Myc were recruited onto the *ALK* promoter region. Schematic drawing of the 5′-upstream region of human *ALK* indicates the positions of putative E-boxes (E1 and E2). Primer sets (F1 R1 and F2 R2) used for ChIP assays are indicated by arrows (top). HeLa cells were transiently transfected with *MYCN* expression plasmid. Forty-eight hours after transfection, ChIP assays were performed using anti-MYCN antibody (middle). To detect the recruitment of endogenous MYCN (bottom left) and c-Myc (bottom right), ChIP assays were carried out in the indicated cell lines using anti-MYCN or anti-c-Myc antibodies. (d) E1 and E2 are important for the transcriptional activation of *ALK*. Site-specific deletions were introduced into the parental core promoter (−350 bp) of the luciferase reporter construct at the indicated E-boxes (left panel). SK-N-AS cells were simultaneously transfected with parental or deletion mutants of luciferase reporter constructs together with *MYCN* or *c-Myc* expression vector. The graph shows the relative luciferase activity driven by the expression of MYC proteins.

contains no PHOX2b binding motif. According to our results, this minimum region of the *ALK* promoter possesses MYC-binding sites and transcriptional activity of *ALK* gene.

More recently, Schonheer *et al.* showed that both wild-type and gain-of-function *ALK* mutants were able to stimulate transcription at the *MYCN* promoter through the activation of a downstream molecule, ERK, and initiate mRNA transcription of *MYCN* in both neuronal and NBL cells[36]. Furthermore, Berry *et al.* demonstrated that the F1174L mutation of ALK enhanced MYCN protein stabilization and found that endogenous *Mycn* mRNA was upregulated in the tumors of *MYCN/ALKF1174L* transgenic mice[37]. Taken together, these data suggest a positive feedback loop for MYCN which, in turn, directly regulates *ALK* expression to potentiate the oncogenic activity of MYCN, leading to rapid malignant transformation.

The theory that ALK overexpression contributes to oncogenic activity is supported by the data obtained from patients with NBL. As described previously, high expression of *ALK* mRNA[25,26] and/or protein[23,24] was significantly correlated with poor outcome of NBL. Consistent with these earlier reports, our present data clearly showed that aggressive and metastatic NBLs (stages 3, 4 and 4s) exhibited a significantly higher expression level of *ALK* mRNA compared with localized and favorable NBLs (stages 1 and 2), suggesting an onco-

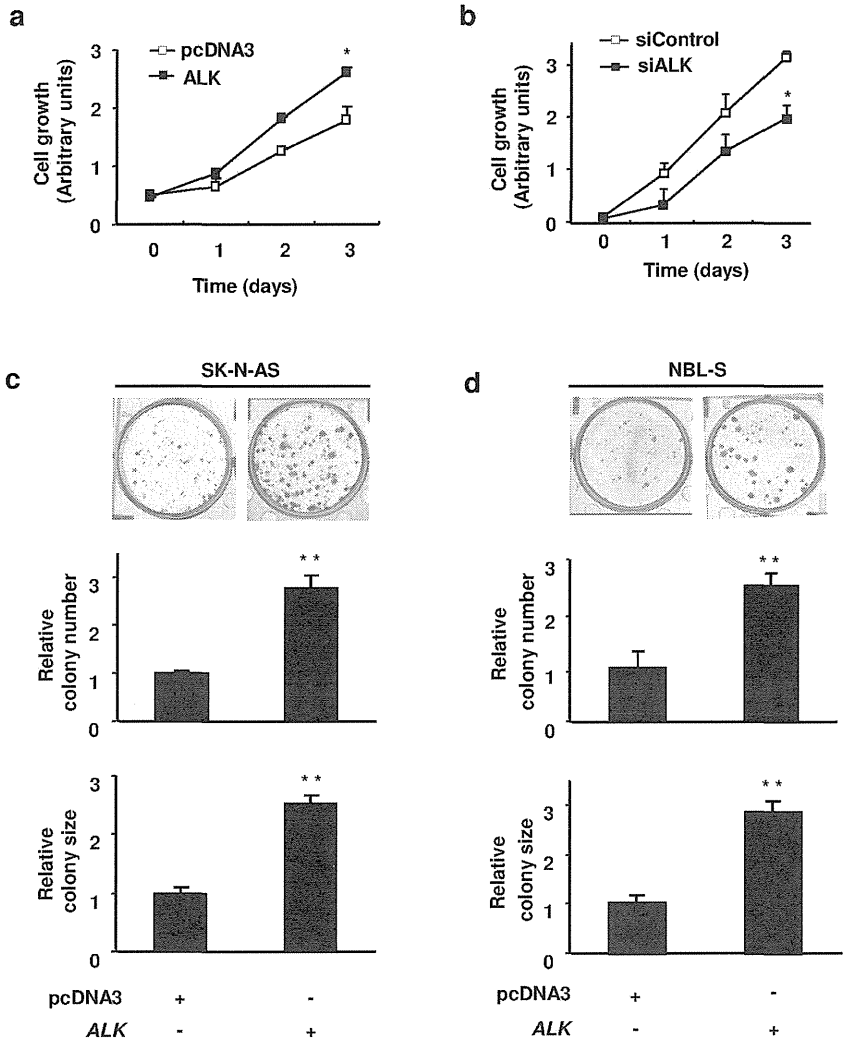

Figure 4 | ALK promotes cell proliferation. (a) SK-N-DZ cells were transfected with the expression plasmid for *ALK* or empty plasmid and subjected to WST-8 assays at the indicated times after transfection. (b) NLF cells were transfected with control siRNA or siRNA against *ALK*. Twenty-four hours after transfection, cells were seeded in 96-well cell culture plates. At the indicated time points, the numbers of viable cells were measured by WST-8 assays. (c) and (d) Colony formation assays. SK-N-AS (c) and NBL-S (d) cells were transfected with pcDNA3-*ALK* or empty plasmid. Forty-eight hours after transfection, cells were transferred to fresh medium containing G418 (400 μg/ml for SK-N-AS and 500 μg/ml for NBL-S cells). Images were taken after crystal violet staining. Numbers and sizes of colonies were counted. All experiments were performed in triplicate.

genic relevance of ALK in NBL. Previously obtained evidence has indicated an important role of ALK in both familial and sporadic NBL pathogenesis[18–22]. However, the contribution of wild-type *ALK* to NBL development was not well understood. Intensive studies have been mainly performed examining a correlation between activating mutations in the tyrosine kinase (TK) domain of *ALK* and poor clinical outcome in NBLs. However, mutations in the TK domain are observed in limited cases. According to De Brouwer and colleagues, only 6.9% missense mutations and 1.7% focal amplifications in *ALK* gene were detected among 709 NBL patients[25]. They have also revealed that there were no significant survival differences observed in tumors with or without *ALK* mutations or amplifications[25], suggesting that wild-type *ALK* might have an important role in NBL pathogenesis. Consistent with Passoni *et al.* and Di Paolo *et al.*, our present findings indicate that wild-type ALK can exert oncogenic activity in NBL cells, in addition to its mutated isoforms.

In the current study, overexpression of either wild-type or mutated *ALK* partially restored the decreased cell proliferation caused by RA treatment, implicating that RA-mediated reduction of *MYCN* expression resulted in decreased cell proliferation partially through the downregulation of *ALK* expression. The contribution of native ALK to migration and invasion implies a role for ALK in tumor progression and metastasis of NBLs. MYCN-induced cell migration was also inhibited by siRNA-mediated knockdown of *ALK*, suggesting that *ALK* is one of the key target genes of MYCN to conduct NBL cell migration. Moreover, treatment with TAE-684 effectively inhibited cell proliferation, migration and invasion of NBL cells with *MYCN* amplification compared to *MYCN*-non-amplified cells. Xenograft tumors derived from *MYCN* amplified NBL cells were significantly suppressed with TAE-684 treatment, indicating that ALK had a pivotal role in the development of NBL with *MYCN* amplification. Taken together, these data provide an important

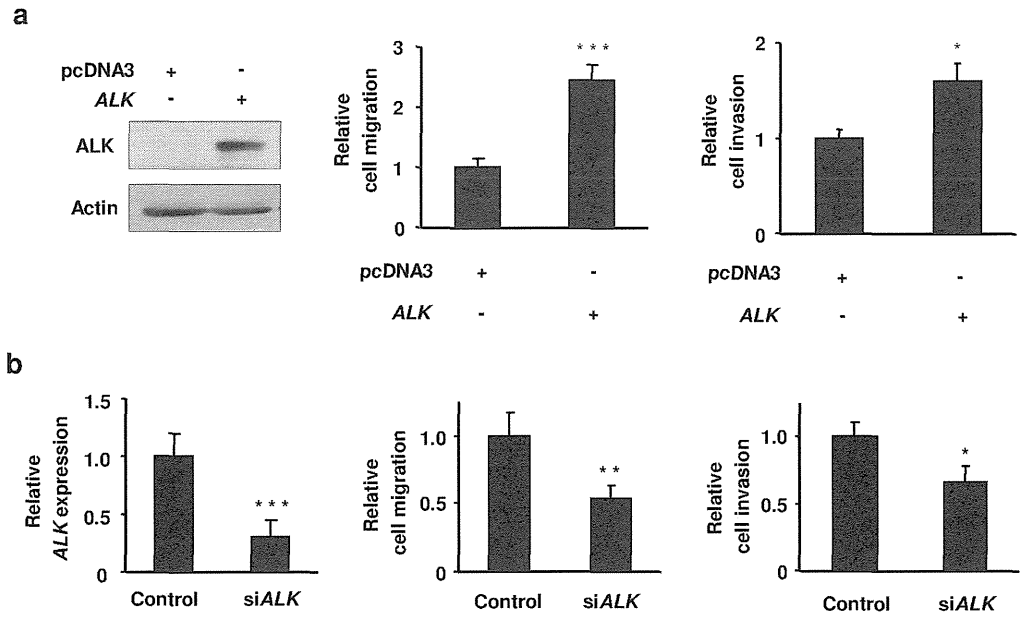

Figure 5 | ALK contributes to cell migration and invasion. (a) Overexpression of ALK enhanced NBL cell migration and invasion. SK-N-AS cells were transfected with pcDNA3-*ALK* or empty plasmid, and ALK ectopic expression (220 kDa) was determined by immunoblotting (left, full-length blots are presented in Supplementary Figure S9). Migration assays (middle) and invasion assays (right) were performed in Boyden chambers. (b) siRNA-mediated knockdown of *ALK* suppressed NBL cell migration and invasion. NBL-S cells were transfected with control siRNA or siRNA targeting *ALK*. Knockdown of *ALK* mRNA expression in NBL-S cells was confirmed by qRT-PCR (left). Migration assays (middle) and invasion assays (right) were performed as (a). All experiments were performed in triplicate.

and direct mechanism by which MYCN is able to sensitize cells and tumors to aggressive characteristics through the regulation of *ALK* expression.

In conclusion, this study provides several lines of evidence that *ALK* is a direct transcriptional target of MYC proteins and a key molecule for MYC proteins to exert influence towards oncogenesis. Thus, our present findings might help to explain a novel molecular mechanism for the development and progression of aggressive NBL with or without *MYCN* amplification, and suggest that a therapy targeting ALK should be considered in combination with more conventional agents to treat NBLs with high expression of ALK.

Methods

Patient population. One hundred and twenty-six patients with NBL were diagnosed clinically and histologically, using surgically removed tumor specimens according to the International Neuroblastoma Pathological Classification (INPC). According to the International NBL Staging System (INSS)[38], 22 patients were diagnosed as stage 1, 12 were stage 2, 23 were stage 3, 63 were stage 4, and 6 were stage 4S. *MYCN* and *ALK* amplification were determined using fluorescence *in situ* hybridization (FISH). This study was approved by the Ethics Committee of the Faculty of Biology and Medicine at the Chiba Cancer Center, and appropriate informed consent was obtained from all patients.

Transgenic mice samples collection and RT-PCR. Tyrosine hydroxylase (TH)-*MYCN* mice were maintained through hemizygotic matings, as previously described[39]. Superior mesenteric ganglion (SMG) tissues were obtained from 2-week-old wild-type or *MYCN*-hemizygous mice (n = 3 mice per group). Adrenal gland tumor tissues were collected from 9-, 10- or 11-week-old *MYCN*-hemizygous mice (n = 3 mice per group). All animals were handled in accordance with institutional guidelines for safe and ethical treatment of mice, and this study was approved by the Animal Care and Use Committee of Nagoya University Graduate School of Medicine. Total RNA extraction was performed using ISOGEN (Nippon Gene, Tokyo, Japan) according to the manufacturer's instructions. cDNA was generated from total RNA using SuperScript III reverse transcriptase and random primers following the manufacturer's recommendations (Invitrogen, Carlsbad, CA, USA). The resultant cDNAs were subjected to PCR-based amplification using the following primer sets and annealing temperatures (Ta): human *MYCN*, 5′-CGACCACAAGGCCCTC AGTA-3′ (sense) and 5′-CAGCCTTGGTGTTGGAGGAG-3′ (antisense), Ta, 56°C; mice *Alk*, 5′-GACAGGATGGCTCCACCACA-3′ (sense) and 5′-CGGAAGCA GAGCGCACACAA-3′ (antisense), Ta, 56°C; mice *Gapdh*, 5′-GGTGGTGAAGCA GGCATCTG-3′ (sense) and 5′-GGAGGCCATGTAGGCCATGA-3′ (antisense), Ta, 57°C.

Cell culture. Human-derived NBL cell lines harboring wild-type *ALK*, including SK-N-AS, SK-N-DZ, NBL-S, NLF, RISA, NB69, SK-N-BE, NMB, NBTU1, NB9, KP-N-NS, SMS-KAN, GOTO, IMR32, GANB, CHP-134, and mutated *ALK*, including SH-SY5Y (F1174L), TNB1 (R1275Q) and SHEP Tet-21/N (F1174L), OAN (D1091N), RTBM1 (F1174L), TGW (R1275Q), SMS-SAN (F1174L), NGP (D1529E), LHN (R1275Q), LAN5 (R1275Q), KCN (R1275Q) and *ALK* amplified NB1 (Amp), were cultivated in RPMI 1640 medium supplemented with 10% heat-inactivated fetal bovine serum (FBS; Invitrogen, Carlsbad, CA, USA) and penicillin (100 IU/ml)/streptomycin (100 μg/ml). Non-NBL cell lines including HeLa, U2OS, A-875, TTC-11, ASPS-KY, RMS-Mk, NOS-1, SAOS-2, OST, G-361, G32TG, A549, H1299, HACAT, HEK-293T, HEK-293, COLO 320, MCF-7 and MDA-MB-453, were maintained in Dulbecco's modified Eagle's medium with the same supplements. Cells were grown at 37°C in a water-saturated atmosphere of 95% air and 5% CO_2. NBL cell lines were obtained from the CHOP cell line bank (Philadelphia, PA, USA). SHEP Tet 21/N cell line was kindly provided by Dr. M. Schwab (German Cancer Research Center, Heidelberg, Germany) and RISA cell line was established at Chiba Cancer Center Research Institute, Chiba, Japan. Non-NBL cell lines were purchased from American Type Culture Collection (ATCC, Manassas, VA, USA). For transient transfection, cells were transfected with the indicated expression of plasmids using Lipofectamine 2000 transfection reagent (Invitrogen), according to the manufacturer's recommendations.

Plasmid constructs. *ALK* promoter construct and different deletion constructs of *ALK* promoter were generated using an In-Fusion HD Cloning Kit (Clontech Laboratories, Mountain View, CA, USA) and inserted into the luciferase pGL4.17-basic plasmid (Promega, Madison, WI, USA). The protein coding region of *c-Myc* was inserted into the pcDNA3 plasmid (Invitrogen). pcDNA3-*ALK* wild-type and pcDNA3-*ALK* (F1174L *ALK* mutation) mutated expression plasmids were kindly provided by Dr. J. Takita (The University of Tokyo, Tokyo, Japan). pUHD-*MYCN* expression plasmid was kindly provided by Dr. M. Schwab (German Cancer Research Center, Heidelberg, Germany). All constructs were verified by DNA sequencing.

RNA isolation and RT-PCR. Total RNA was prepared from the indicated cell lines using an RNeasy Mini Kit (Qiagen, Valencia, CA, USA) according to the manufacturer's recommendations. cDNA was generated from total RNA using SuperScript II reverse transcriptase and random primers following the manufacturer's conditions (Invitrogen). The resultant cDNAs were subjected to PCR-based amplification using the following primer sets and annealing temperatures

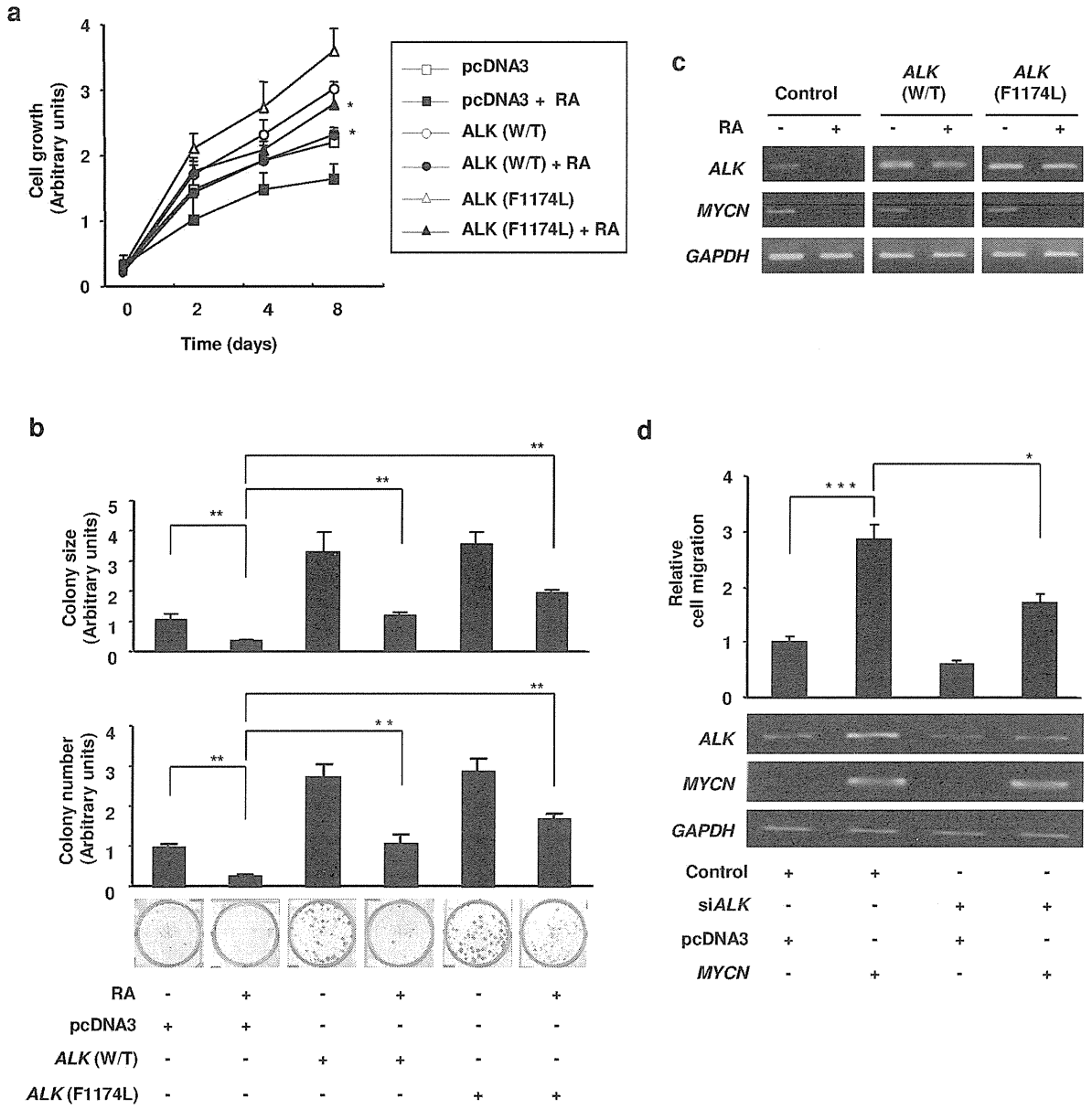

Figure 6 | MYCN induces oncogenesis through regulating ALK expression. (a) and (b) Effect of RA on the proliferative and colony forming abilities of NBL cells overexpressing *ALK*. Cell proliferation assays (a) and colony formation assays (b) to examine the proliferation of GOTO cells with wild-type or F1174L mutated *ALK* showed a significant difference in cell proliferation following treatment with RA (10 μM). (c) GOTO cells were transfected with pcDNA3-*ALK* (wild-type or mutated) or empty plasmid. Twenty-four hours after transfection, cells were treated with or without RA. Forty-eight hours after RA treatment, the expression of *ALK* and *MYCN* mRNA was verified by RT-PCR. (d) Cell migration assay. NBL-S cells were transfected with siRNA against *ALK*, followed by the transfection of *MYCN* expression vector or empty vector 24 h after siRNA transfection. Seventy-two hours after the first transfection, cell migration was examined (upper panel) and the expression levels of *ALK* and *MYCN* were determined (lower panel) by RT-PCR. All experiments were performed in triplicate.

(Ta): human *MYCN*, 5′- CTTCGGTCCAGCTTTCTCAC-3′ (sense) and 5′- GTCC GAGCGTGTTCAATTTT-3′ (antisense), Ta, 58°C; human *GAPDH*, 5′-ACCTGA CCTGCCGTCTAGAA-3′ (sense) and 5′-TCCACCACCCTGTTGCTGTA-3′ (antisense), Ta, 58°C; human *ALK*, 5′-AGGACCCGGATGTAATCAAC-3′ (sense) and 5′- CTTGTGCAACTCCGAAGGAG-3′ (antisense), Ta, 58°C; human *c-Myc*, 5′- CTCGACTACGACTCGGTGCA-3′ (sense) and 5′ TGGTGGGCGGTGTCTCCT CA-3′ (antisense), Ta, 60°C. To control for the integrity and uniformity of the sample preparation, *GAPDH* mRNA was amplified. All PCR amplifications were carried out with a GeneAmp PCR 9700 (Applied Biosystems, Foster City, CA, USA), using rTaq DNA polymerase (Takara, Shiga, Japan). PCR products were separated by 2.0% agarose gel electrophoresis and stained with ethidium bromide.

Quantitative real-time PCR (qRT-PCR). Total RNA was extracted from clinical samples and NBL as well as non-NBL cell lines using TRIzol reagent (Invitrogen) according to the manufacturer's instructions, and reverse transcription was performed with SuperScript II reverse transcriptase (Invitrogen). qRT-PCR was carried out using an ABI Prism 7700 sequence detection system (Applied Biosystems), according to the manufacturer's protocol. TaqMan probe for *ALK*

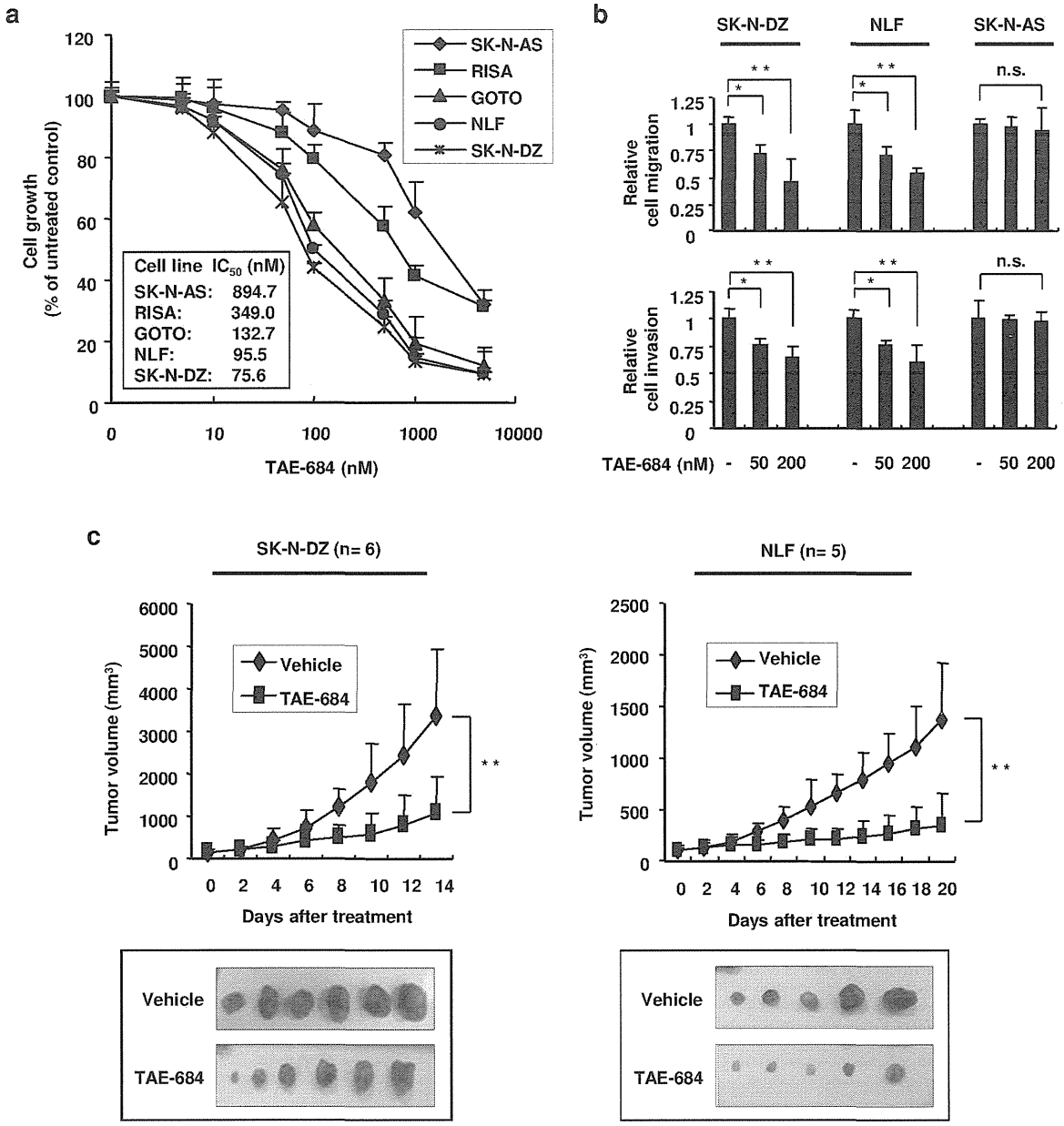

Figure 7 | Effects of ALK inhibitor TAE-684 on NBL cells and xenograft tumors. (a) TAE-684 reduced the proliferation of NBL cells. *MYCN*-non-amplified (SK-N-AS and RISA) or amplified (GOTO, NLF and SK-N-DZ) NBL cells were cultured with varying concentrations of TAE-684 for 72 h and cell proliferation was measured. The values are mean ± SD of triplicate experiments. (b) TAE-684 suppressed cell migration and invasion of NBL cells with *MYCN* amplification. NBL cells with *MYCN* amplification (SK-N-DZ and NLF) or without amplification (SK-N-AS) were treated with 50 nM or 200 nM of TAE-684 or DMSO as control, and cell migration (upper panel) or invasion (lower panel) assays were performed. The values are mean ± SD of triplicate experiments. (c) TAE-684 suppressed tumor growth in mice. SK-N-DZ (left panel) and NLF (right panel) cells were subcutaneously injected into mice. When palpable tumors appeared, mice were orally treated with TAE-684 or carrier solution (vehicle), and tumor sizes were measured. Tumor sizes are displayed as mean ± SD at the indicated time interval of TAE-684 treatment (upper panel). Pictures of subcutaneous tumors for each group are shown (lower panel). n = 6 for each group of SK-N-DZ cells and n = 5 for each group of NLF cells.

(Assay ID: Hs00608292_m1) and β-actin control reagent kit were purchased from Applied Biosystems. *MYCN* mRNA expression was measured by the SYBR green real-time PCR system using the following primer set: 5′-GGACACCCTGAGCG ATTCAGA-3′ (sense) 5′-AGGAGGAACGCCGCTTCT-3′ (antisense). The mRNA levels of each gene were standardized by β-actin.

siRNA-mediated knockdown. Cells were transiently transfected with 10 nM siRNA targeting *MYCN*, siRNA-1: 5′-GAACCCAGACCUCGAGUUUUU-3′ (sense); 5′-PAAACUCGAGGUCUGGGUUCUU-3′ (antisense) and siRNA-2: 5′-UCACGG AGAUGCUGCUUGAUU-3′ (sense), 5′-PUCAAGCAGCAUCUCCGUGAUU-3′ (antisense) or a control non-targeting siRNA (Thermo Fisher Scientific, Waltham, MA, USA) using Lipofectamine RNAiMAX transfection reagent (Invitrogen) according to the manufacturer's instructions. Seventy-two hours after transfection, total RNA was prepared and subjected to RT-PCR. To knockdown endogenous *ALK* expression, cells were transfected with 100 nM of control siRNA or with siRNA against *ALK* target sequences: 5′-CCUGUAUACCGGAUAAUGA-3′,

5′-GUUGGGGUCAUAGAUGUUU-3′, 5′-UGAUUAUUUUACAUGGAAU-3′, 5′-GGAGGUGGCUGGAAUGAUA-3′ (Thermo Fisher Scientific) according to the manufacturer's recommendations. Seventy-two hours after transfection, cell lysates were prepared and analyzed for *ALK* and *GAPDH* expression levels by qRT-PCR or the expression levels of ALK, pALK, AKT and pAKT by immunoblotting analysis.

Site-specific deletion. The luciferase reporter constructs (−350 bp)-Δ E1 and (−350 bp)-ΔE 1/2 deletion constructs were generated with QuikChange Site-Directed Mutagenesis System (Invitrogen) on the basis of the parental construct (−350 bp), according to the manufacturer's instructions. The following primer sets were used: (−350 bp)–ΔE1, 5′-GCGCGGCTCAGCCAGCTGGCGGGCGCCCAG-3′ (sense) and 5′-CATCTGCCTGGGCGCCCGCCAGCTGGCTGAG-3′ (antisense); (−350 bp)–ΔE2, 5′-GCAGCAGCGCGGAGTTGGAGCCCCGCCCC-3′ (sense) and 5′-CCCGGAGGGGGCGGGGCTCCAACTCCGCG-3′ (antisense). The deletions were verified by DNA sequencing.

Luciferase reporter assays. Cells (5×10^4) were seeded in 12-well cell culture plates (Becton Dickinson, NJ, USA) and allowed to adhere overnight. Cells were then co-transfected with expression plasmid, luciferase reporter construct and pRL-TK Renilla luciferase cDNA. Total amounts of plasmid DNA per transfection were kept constant with empty plasmid pcDNA3 and/or pGL4.17. Forty-eight hours after transfection, cells were lysed, and both firefly and Renilla luciferase activities were measured with the Dual-Luciferase Reporter Assay system (Promega), according to the manufacturer's instructions. The firefly luminescence signal was normalized based on the Renilla luminescence signal.

ChIP assays. Chromatin immunoprecipitation (ChIP) assays were performed using a chromatin immunoprecipitation assay kit according to the protocol provided by Millipore (Bedford, MA, USA). In brief, TNB1 (high *ALK* expression), RISA (low *ALK* expression), A-875 (high *ALK* expression) and HeLa cells (low *ALK* expression) were cross-linked with formaldehyde, and cross-linked chromatin was sonicated followed by immunoprecipitation with anti-IgG (Cell Signaling), polyclonal anti-MYCN and/or monoclonal anti-c-Myc (anti-MYC-Tag (9B11)) antibody. DNA of the immunoprecipitates and control input DNA were purified and then analyzed by standard PCR using the following primer sets: F1 (−350), 5′-GCTCGCTAGCCTC GAAGTTCTCACATTTGCTCC-3′ (sense); R1 (+30), 5′- TCTTGATATCCTCG AGTACCAGCTGCTACC-3′ (antisense) and F2(-1813), 5′-GGAGAGGGGTATTA TTAGAGAACG-3′ (sense); R2 (−1433), 5′- GGGCAAAGAATTATCTCACCC- 3′ (antisense).

Cell proliferation assays. Cells (1×10^3) were seeded in 96-well cell culture plates (Becton Dickinson, NJ, USA) and allowed to adhere overnight. At the indicated time points, cell proliferation was measured using a cell counting kit-8 (Dojindo, Kumamoto, Japan) according to manufacturer's instructions.

Colony formation assays. Cells were seeded at a final density of 2×10^4 cells per well in 6-well cell culture plates (Becton Dickinson, NJ, USA) and allowed to attach overnight. Cells were then transfected with the empty or pcDNA3-*ALK* expression plasmid. Forty-eight hours after transfection, cells were transferred to the fresh medium containing G418. After 14 days, viable colonies were washed in PBS, fixed with 4% paraformaldehyde (PFA) and stained with crystal violet solution.

Retinoic acid treatment. To study the effect of retinoic acid (RA, Sigma, St. Louis, MO, USA) on the proliferation or colony formation of GOTO cells expressing wild-type or mutated *ALK*, transfected cells were grown in normal growth medium, and dimethylsulfoxide (DMSO) or 10 μM RA (with 50 μg/ml of G418 for colony formation assays) was added to the medium the following day. The culture medium was changed every 48 h to replenish the RA and G418. Cell viability and colony formation assays were performed as described above.

Cell migration and invasion assays. Cell motility was measured using 8-μm pore size FluoroBlok Transwell chambers (BD Biosciences, San Diego, CA, USA). Cells were collected by a brief treatment with trypsin/EDTA solution, washed once with serum-containing medium, centrifuged, resuspended in medium containing 0.1% bovine serum albumin, and then placed in the inserts at a concentration of 2.5×10^4 cells in 250 μl (migration assays) or 5×10^4 cells in 250 μl (invasion assays). In the lower compartments of the chambers, 750 μl of medium containing 10% FBS was added as a chemoattractant. Invasion assays were carried out by the same procedure except that the filters of the Transwell chambers were coated with 50 μg Matrigel (BD Biosciences). After incubation at 37°C for 16 h (migration assays) or 24 h (invasion assays), cells that migrated through the pores to the lower chamber were stained with Giemsa solution or 1 μM Calcein AM (Invitrogen). Stained cells were analyzed by either counting under the microscope or by detecting the fluorescence intensity using microplate reader (Perkin-Elmer, Waltham, MA, USA).

Immunoblot analysis. Immunoblotting was performed as previously described[40] using the following antibodies: monoclonal anti-ALK was from Beckman Coulter (Marseille, France), polyclonal anti-phosphorylated Tyr-1604 ALK, polyclonal anti-AKT, polyclonal anti-phosphorylated AKT Ser-473, polyclonal anti-MYCN and monoclonal anti-MYC-Tag (9B11) were from Cell Signaling (Danvers, MA, USA), polyclonal anti-Actin was from Sigma-Aldrich (St. Louis, MO, USA). All antibodies were used at a dilution of 1 : 1000 in immunoblot analysis.

Drug treatment. ALK inhibitors, TAE-684[41,42] and CH5424802[43] were purchased from Active Biochemicals (Hong Kong, China), and crizotinib[36,37,44] was purchased from Selleck (Houston, TX, USA). For cell proliferation assay; NBL cells (3×10^3) were seeded in 96-well cell culture plates and treated with varying concentrations of TAE-684, crizotinib or CH5424802 for 72 h and cell proliferation was measured as described above. The IC_{50} (half maximal inhibitory concentration) values of NBL cells were calculated by nonlinear regression (variable slope) using the GraphPad Prism 6 software (La Jolla, CA, USA). Cell migration and invasion assay; cell migration and invasion assays were performed as described above with or without the treatment of 50 nM or 200 nM of TAE-684, crizotinib or CH5424802.

Xenograft study; NBL cells with *MYCN* amplification (SK-N-DZ and NLF) were subcutaneously injected (5×10^6 cells/inoculate in RPMI 1640 together with an equal volume of Matrigel, Becton Dickinson) in the right flank of C.B-17-SCID female mice at 6 weeks old. After implantation, tumor sizes were measured using the following formula: [(width)^2 × length]/2. Treatment of TAE-684 was initiated at the time when tumor size exceeds 85 mm^3. TAE-684 was resuspended in 10% N-methyl-2-pyrrolidinone (Wako, Osaka, Japan)- 90% PEG (polyethylene glycol, molecular weight 300) (Wako) solution. Mice were administered TAE-684 (10 mg/kg) by oral gavage once daily. All mice were housed in a pathogen-free conditions strictly following the Chiba Cancer Center Research Institute guidelines, and these studies were approved by the Institutional Animal Care and Use Committee of Chiba Cancer Center Research Institute.

Data analysis. Results were expressed as the mean ± SD. Student's *t* tests and two-independent samples *t* tests were used to compare the differences in the means of different groups. *P* values of <0.05 were considered statistically significant. *P* values of <0.05, <0.01 and <0.001 were denoted by a single asterisk, double asterisks and triple asterisks, respectively. n.s. indicates not significant at the 0.05 probability level.

1. Brodeur, G. M. Neuroblastoma: biological insights into a clinical enigma. *Nat. Rev. Cancer* **3**, 203–216 (2003).
2. Nakagawara, A. *et al.* Association between high levels of expression of the TRK gene and favorable outcome in human neuroblastoma. *N. Engl. J. Med.* **328**, 847–854 (1993).
3. Ogawa, S., Takita, J., Sanada, M. & Hayashi, Y. Oncogenic mutations of ALK in neuroblastoma. *Cancer Sci.* **102**, 302–308 (2011).
4. Brodeur, G. M., Seeger, R. C., Schwab, M., Varmus, H. E. & Bishop, J. M. Amplification of N-myc in untreated human neuroblastomas correlates with advanced disease stage. *Science* **224**, 1121–4 (1984).
5. Seeger, R. C. *et al.* Association of multiple copies of the N-myc oncogene with rapid progression of neuroblastomas. *N. Engl. J. Med.* **13**, 1111–6 (1985).
6. Kohl, N. E., Gee, C. E. & Alt, F. W. Activated expression of the N-myc gene in human neuroblastomas and related tumors. *Science* **226**, 1335–7 (1984).
7. Riley, R. D. *et al.* A systematic review of molecular and biological tumor markers in neuroblastoma. *Clin. Cancer Res.* **10**, 4–12 (2004).
8. Lutz, W. *et al.* Conditional expression of N-myc in human neuroblastoma cells increases expression of alpha-prothymosin and ornithine decarboxylase and accelerates progression into S-phase early after mitogenic stimulation of quiescent cells. *Oncogene* **13**, 803–12 (1996).
9. Bernards, R., Dessain, S. K. & Weinberg, R. A. N-myc amplification causes down-modulation of *MHC* class I antigen expression in neuroblastoma. *Cell* **47**, 667–74 (1986).
10. Goodman, L. A. *et al.* Modulation of N-*myc* expression alters the invasiveness of neuroblastoma. *Clin. Exp. Met.* **15**, 130–139 (1997).
11. Tanaka, N. & Fukuzawa, M. MYCN downregulates integrin alpha1 to promote invasion of human neuroblastoma cells. *Int. J. Oncol.* **33**, 815–2 (2008).
12. Weiss, W. A., Aldape, K., Mohapatra, G., Feuerstein, B. G. & Bishop, J. M. Targeted expression of MYCN causes neuroblastoma in transgenic mice. *EMBO J.* **16**, 2985–95 (1997).
13. Alex, R., Sozeri, O., Meyer, S. & Dildrop, R. Determination of the DNA sequence recognized by the bHLH-zip domain of the N-Myc protein. *Nucleic Acids Res.* **20**, 2257–63 (1992).
14. Blackwood, E. M. & Eisenman, R. N. Regulation of Myc: Max complex formation and its potential role in cell proliferation. *Tohoku J. Exp. Med.* **168**, 195–202 (1992).
15. Torres, R., Schreiber-Agus, N., Morgenbesser, S. D. & DePinho, R. A. Myc and Max: a putative transcriptional complex in search of a cellular target. *Curr. Opin. Cell Biol.* **4**, 468–74 (1992).
16. De Preter, K. *et al.* Human fetal neuroblast and neuroblastoma transcriptome analysis confirms neuroblast origin and highlights neuroblastoma candidate genes. *Genome Biol.* **7**, R84 (2006).
17. Osajima-Hakomori, Y. *et al.* Biological role of anaplastic lymphoma kinase in neuroblastoma. *Am. J. Pathol.* **167**, 213–22 (2005).
18. Chen, Y. *et al.* Oncogenic mutations of ALK kinase in neuroblastoma. *Nature* **455**, 971–974 (2008).
19. George, R. E. *et al.* Activating mutations in ALK provide a therapeutic target in neuroblastoma. *Nature* **455**, 975–978 (2008).
20. Janoueix-Lerosey, I. *et al.* Somatic and germline activating mutations of the ALK kinase receptor in neuroblastoma. *Nature* **455**, 967–970 (2008).
21. Mosse, Y. P. *et al.* Identification of ALK as a major familial neuroblastoma predisposition gene. *Nature* **455**, 930–5 (2008).

22. Caren, H., Abel, F., Kogner, P. & Martinsson, T. High incidence of DNA mutations and gene amplifications of the ALK gene in advanced sporadic neuroblastoma tumours. *Biochem. J.* **416**, 153–159 (2008).
23. Passoni, L. *et al.* Mutation- independent anaplastic lymphoma kinase overexpression in poor prognosis neuroblastoma patients. *Cancer Res.* **69**, 7338–7346 (2009).
24. Duijkers, F. A. *et al.* High anaplastic lymphoma kinase immunohistochemical staining in neuroblastoma and ganglioneuroblastoma is an independent predictor of poor outcome. *Am. J. Pathol.* **180**, 1223–3 (2012).
25. De Brouwer, S. *et al.* Meta-analysis of neuroblastomas reveals a skewed ALK mutation spectrum in tumors with MYCN amplification. *Clin. Cancer Res.* **16**, 4353–62 (2010).
26. Schulte, J. H. *et al.* High ALK receptor tyrosine kinase expression supersedes ALK mutation as a determining factor of an unfavorable phenotype in primary neuroblastoma. *Clin. Cancer Res.* **17**, 5082–92 (2011).
27. Di Paolo, D. *et al.* Selective therapeutic targeting of the anaplastic lymphoma kinase with liposomal siRNA induces apoptosis and inhibits angiogenesis in neuroblastoma. *Mol. Ther.* **19**, 2201–12 (2011).
28. Banerjee, S. A., Hoppe, P., Brilliant, M. & Chikaraishi, D. M. 5′ Flanking sequences of the rat tyrosine hydroxylase gene target accurate tissue-specific, developmental, and trans synaptic expression in transgenic mice. *J. Neurosci.* **12**, 4460–4467 (1992).
29. Akter, J. *et al.* Expression of NLRR3 orphan receptor gene is negatively regulated by MYCN and Miz-1, and its downregulation is associated with unfavorable outcome in neuroblastoma. *Clin. Cancer Res.* **17**, 6681–92 (2011).
30. Moog-Lutz, C. *et al.* Activation and inhibition of anaplastic lymphoma kinase receptor tyrosine kinase by monoclonal antibodies and absence of agonist activity of pleiotrophin. *J. Bio. Chem.* **280**, 26039–26048 (2005).
31. Thiele, C. J., Reynolds, C. P. & Israel, M. A. Decreased expression of N-myc precedes retinoic acid-induced morphological differentiation of human neuroblastoma. *Nature* **313**, 404–406 (1985).
32. Ichimiya, S. *et al.* Downregulation of hASH1 is associated with the retinoic acid-induced differentiation of human neuroblastoma cell lines. *Med. Pediatr. Oncol.* **36**, 132–4 (2001).
33. Futami, H. & Sakai, R. All-trans retinoic acid downregulates ALK in neuroblastoma cell lines and induces apoptosis in neuroblastoma cell lines with activated ALK. *Cancer Let.* **297**, 220–225 (2010).
34. Grandori, C. & Eisenman, R. N. Myc target genes. *Trends Biochem. Sci.* **22**, 177–181 (1997).
35. Bachetti, T. *et al.* PHOX2B-mediated regulation of ALK expression: in vitro identification of a functional relationship between two genes involved in neuroblastoma. *PLoS One* **5**, e13108 (2010).
36. Schonheer, C. *et al.* Anaplastic Lymphoma Kinase (ALK) regulates initiation of transcription of *MYCN* in neuroblastoma cells. *Oncogene* **31**, 5193–5200 (2012).
37. Berry, T. *et al.* The ALK^{F1174L} mutation potentiates the oncogenic activity of MYCN in neuroblastoma. *Cancer Cell* **22**, 117–130 (2012).
38. Brodeur, G. M. *et al.* Revisions of the international criteria for neuroblastoma. Diagnosis, staging, and response to treatment. *J. Clin. Oncol.* **11**, 1466–77 (1993).
39. Huang, P. *et al.* The neuronal differentiation factor NeuroD1 downregulates the neuronal repellent factor Slit2 expression and promotes cell motility and tumor formation of neuroblastoma. *Cancer Res.* **71**, 2938–48 (2011).
40. Hossain, S. *et al.* NLRR1 enhances EGF-mediated *MYCN* induction in neuroblastoma and accelerates tumor growth in vivo. *Cancer Res.* **72**, 4587–96 (2012).
41. Galkin, A. V. *et al.* Identification of NVP-TAE684, a potent, selective, and efficacious inhibitor of NPM-ALK. *Proc. Natl. Acad. Sci. USA* **104**, 270–275 (2007).
42. Heukamp, L. C. *et al.* Targeted expression of mutated ALK induces neuroblastoma in transgenic mice. *Sci. Trans. Med.* **4**, 141ra91 (2012).
43. Sakamoto, H. *et al.* CH5424802, a selective ALK inhibitor capable of blocking the resistant gatekeeper mutant. *Cancer Cell* **19**, 679–690 (2011).
44. Christensen, J. G. *et al.* Cytoreductive antitumor activity of PF-2341066, a novel inhibitor of anaplastic lymphoma kinase and c-Met, in experimental models of anaplastic large-cell lymphoma. *Mol. Cancer Ther.* **6**, 3314–22 (2007).

Acknowledgments

We are grateful to Dr. N. Koshikawa and Mr. M. A. Rahman (Chiba Cancer Center Research Institute, Japan) for their excellent technical advice and to Dr. A. Nakazawa (National Center for Child Health and Development, Japan) for useful discussions. We also thank Drs. M. Atwa, H. G. A. El_Azeem and E. El_Gezawy (Assiut University, Egypt) for their important suggestions. This work was supported in part by a Grant-in-Aid from the Ministry of Health, Labour and Welfare for the Third Term Comprehensive Control Research for Cancer (A. Nakagawara), a Grant-in-Aid for JSPS KAKENHI Grant Number 24249061 and 21390317 (A. Nakagawara), Takeda Science Foundation (A. Nakagawara) and grant-in-aids from the National Cancer Center Research and Development Fund, Japan (K. Kadomatsu and A. Nakagawara).

Author contributions

M.K.H. and As.N. designed, performed and analyzed cellular and animal experiments, clinical data, and wrote the manuscript. A.T. performed and analyzed cellular and animal experiments, and wrote the manuscript. S.K. and K.K. performed and analyzed animal experiments and wrote the manuscript. M.O. performed and analyzed clinical data. Y.S., S.H., J.A., A.O. and Y.N. assisted in the experiments and figures. Ak.N. designed and supervised the experiments, analyzed data, wrote and edited the manuscript.

Additional information

Supplementary information accompanies this paper at http://www.nature.com/scientificreports

Competing financial interests: The authors declare no competing financial interests.

How to cite this article: Hasan, M.K. *et al. ALK* is a MYCN target gene and regulates cell migration and invasion in neuroblastoma. *Sci. Rep.* 3, 3450; DOI:10.1038/srep03450 (2013).

Oshiro et al. Radiation Oncology 2013, 8:142
http://www.ro-journal.com/content/8/1/142

RADIATION ONCOLOGY

RESEARCH Open Access

Clinical results of proton beam therapy for advanced neuroblastoma

Yoshiko Oshiro[1], Masashi Mizumoto[1], Toshiyuki Okumura[1], Shinji Sugahara[4], Takashi Fukushima[2], Hitoshi Ishikawa[1], Tomohei Nakao[2], Takayuki Hashimoto[1], Koji Tsuboi[1], Haruo Ohkawa[3], Michio Kaneko[3] and Hideyuki Sakurai[1*]

Abstract

Purpose: To evaluate the efficacy of proton beam therapy (PBT) for pediatric patients with advanced neuroblastoma.

Methods: PBT was conducted at 21 sites in 14 patients with neuroblastoma from 1984 to 2010. Most patients were difficult to treat with photon radiotherapy. Two and 6 patients were classified into stages 3 and 4, respectively, and 6 patients had recurrent disease. Seven of the 8 patients who received PBT as the initial treatment were classified as the high risk group. Twelve patients had gross residual disease before PBT and 2 had undergone intraoperative radiotherapy before PBT. Five patients received PBT for multiple sites, including remote metastases. Photon radiotherapy was used in combination with PBT for 3 patients. The PBT doses ranged from 19.8 to 45.5 GyE (median: 30.6 GyE).

Results: Seven patients are alive with no evidence of disease, 1 is alive with disease progression, and 6 died due to the tumor. Recurrence in the treatment field was not observed and the 3-year locoregional control rate was 82%. Severe acute radiotoxicity was not observed, but 1 patient had narrowing of the aorta and asymptomatic vertebral compression fracture at 28 years after PBT, and hair loss was prolonged in one patient.

Conclusion: PBT may be a better alternative to photon radiotherapy for children with advanced neuroblastoma, and may be conducted safely for patients with neuroblastoma that is difficult to manage using photon beams.

Keywords: Neuroblastoma, Proton therapy, Radiotherapy, Late toxicity, Pediatrics

Introduction

Neuroblastoma is the most common extracranial solid tumor in children. Half of newly diagnosed patients present with high risk disease that is widely metastatic and has large and invasive lesions in the advanced stage. Aggressive treatment is conducted in these cases because they are highly sensitive to radiotherapy and chemotherapy. However, despite recent progress with systemic therapy, the treatment outcome in high risk neuroblastoma is poor [1-5]. Advanced neuroblastoma also often recurs and the prognosis after recurrence is extremely poor [6-8], with Garaventa et al. finding survival rates of only 6.6% and 1.5% in patients with progression and relapse disease [7]. Recently, the superiority of the dose distribution in proton beam therapy (PBT) has been shown compared to the photon dose distribution especially in children [9-13]. However, to our knowledge, there are few reports on clinical outcomes after PBT. [14] We have mainly treated patients with advanced high risk neuroblastoma or recurrent disease using PBT since 1984. Herein, we report a retrospective review of the outcome and toxicity in these patients.

Methods

Patients

Fourteen patients with neuroblastoma received PBT at 21 sites from 1984 to 2010 at our institute. The patient characteristics are shown in Table 1. The patients were 6 boys and 8 girls with a median age of 3 years old (range 1 to 6 years old). PBT was conducted because photon beam radiotherapy was difficult due to a large irradiation area involving normal organs such as the liver, heart, and gastrointestinal tract for 8 patients (Nos. 1–3, 6, 7,

* Correspondence: hsakurai@pmrc.tsukuba.ac.jp
[1]Department of Radiation Oncology, University of Tsukuba, Tennodai 1-1-1, Tsukuba, Ibaraki, Japan
Full list of author information is available at the end of the article

Table 1 Background of 14 patients treated with proton beam therapy

Patient No	Age at PBT	Risk	INSS stage	Site	Surgery	Gross residual disease at PBT	PBT dose (GyE)	Port No.	Sedation	Respiratory gating	X-ray
1	1	Unknown	3	upper abdomen	open biopsy	Yes	28.6	1	yes	no	none
2	2	High	4	retroperitoneum	complete resection	No	19.8	1	yes	yes	Photon for femoral bone
3	6	High	3	mediastinum	None	Yes	30.6	3	no	yes	Electron for axillary LN and skull
4	5	High	3	Paranasal sinus	None	No	19.8	2	no	no	Photon for whole neck LN
5	3	High	4	paravertebra	partial removal	Yes	39.6	1	no	yes	none
6	3	High	4	retroperitoneum	partial removal	Yes	30.6	2	no	yes	none
7	5	High	4	retroperitoneum	partial removal	Yes	30.6	2	no	yes	none
				skull base	None	No	19.8	2		no	
8	2	High	4	retroperitoneum	partial removal	No	19.8	2	yes	yes	none
				skull	None	Yes	19.8	1		no	
				orbit	None	Yes	19.8	1		no	
9	3	High	R*	orbit	none	Yes	43.7	1	yes	no	Cobalt for neck LN
10	6	High	R	paravertebra	None	Yes	45.5	2	no	no	none
				mediastinal node	None	Yes	45.5	2		yes	
11	6	High	R	skull base	None	Yes	33.7	2	no	no	none
				occipital bone	None	Yes	33.7	2		no	
12	2	Intermediate	R	retroperitoneum	none	Yes	41.4	2	yes	yes	Post IORT 12Gy
13	2	High	R	retroperitoneum	None	Yes	41.4	2	yes	yes	Post IORT 12Gy
14	6	Intermediate	R	paraaorta LN†	None	Yes	30.6	2	no	yes	none
				supraclavicular LN	None	Yes	30.6	1		no	
				acetabulum	None	Yes	30.6	2		no	

*R: recurrent disease, †LN: lymph nodes.

12–14), and because PBT was considered a better option for reduction of the dose to the eyes for 4 patients with orbital, paranasal sinus and skull base disease (Nos. 4, 8, 9, 11). The other 2 patients (Nos. 5, 10) received PBT because of the wishes of their families. All patients had received chemotherapy before PBT.[2] Eight patients received PBT as initial treatment, including two with Stage 3 and six with Stage 4 disease classified by the International Neuroblastoma Staging System (INSS). The other 6 patients received PBT for recurrent disease. Twelve patients of the 14 had gross residual disease. Eleven patients were classified as high risk (i.e. those with stage 4 disease aged older than 1 year at diagnosis or those with stage 3 MYCN-amplified tumors), 2 with recurrent disease were intermediate risk (i.e. stage 3 disease aged older than 1 year with favorable histology and MYCN-non-amplified tumors), and insufficient biological and histological data were available to determine the risk group in 1 patient diagnosed in 1982 according to the international neuroblastoma risk group (INRG) staging system[15]. The treatment site was the abdomen and pelvis in 9 cases, head and neck in 7, thorax in 2, paravertebra in 1, acetabulum in 1, and skull in 1. Five patients received PBT at multiple sites for primary and metastatic lesions. Photon radiotherapy was used in combination with PBT for 3 patients for lymph nodes and distant metastases. Intraoperative radiotherapy (IORT) had undergone for the recurrent disease in 2 patients.

Proton therapy

Before treatment, CT images for PBT planning were obtained at intervals of 2–5 mm in the treatment position. The interval was determined based on the patient's age, height and treatment site. For 10 patients with pelvic and thoracic disease, the CT image was obtained during the end expiratory phase using a respiratory gating system, as described previously [16,17]. The gross tumor volume (GTV) was defined as the tumor volume after remission induction chemotherapy for a primary tumor and the tumor volume before PBT for a recurrent tumor. The clinical target volume (CTV) was defined as the GTV plus a 1.5-cm margin and the PTV was defined as the CTV plus a 0.5- to 0.7-cm margin, in principle; however, the balance between toxicity and treatment effect was also taken into account in determining the CTV. Sedatives were administered for 5 patients aged 1 to 3 for planning CT and treatment.

Between 1994 and 2000, PBT was limited to 4 hours a day and 120 days a year according to proton beam availability from the National Laboratory for High Energy Physics. Beam lines were also limited to fixed vertical and horizontal beam lines, and patients were immobilized by Styrofoam box manually-hollowed out for individuals. From September 2001, the new hospital-based facility which includes rotational gantries, releases adequate energy proton beams from any direction, using the respiratory gating for 10 patients with pelvic and thoracic disease with the body immobilized using an individually shaped body cast (ESFORM; Engineering System Co., Matsumoto). Patients with head and neck tumors were also immobilized using individually manufactured thermoplastic masks. The treatment is provided 5 days in a week. Respiratory gating was used for the 10 patients with pelvic and thoracic disease. The photon equivalent dose (GyE) was defined as the physical dose (Gy) × the relative biological effectiveness of the proton beam assigned a value of 1.1. Before each treatment, correct placement of the patient relative to the radiation field was confirmed fluoroscopically. The given doses ranged from 19.8 to 45.5 GyE (median: 30.6 GyE) in 11 to 23 fractions. In Japan, the common dose for neuroblastoma with a complete response after chemotherapy is 19.8 Gy, and 10.8 Gy was added for grossly residual disease. In this series, higher doses were administered for patients with recurrent and chemotherapy-resistant disease. Patients underwent a routine physical examination once a week during PBT. After completion of PBT, patients were followed in combination with a pediatrician using CT, MRI, ^{99m}Tc bone scans, and ^{131}I- and ^{123}I- metaiodobenzylguanidine scintigrams.

Statistical analysis

Locoregional failure was defined as tumor progression in the anatomic compartment that contained the primary tumor (pelvis, abdomen, thorax, neck). The locoregional control rate was calculated from the start of PBT to the date of local failure in the irradiation field, marginal recurrence, or most recent local progression-free follow up. Statistical analyses were performed using SPSS software (SPSS Inc., Chicago, IL, USA). Acute and late toxicities associated with treatments were evaluated using the National Cancer Institute Common Toxicity Criteria for Adverse Events (CTCAE) version 4.0.

Results

The results for the 14 patients are shown in Table 2. The median follow-up periods from diagnosis and the start of PBT were 40 months (M) (range: 17 M-30 years (Y)) and 21 M (5 M-29 Y), respectively, for all patients, and 46 M (25 M-30 Y) and 30 M (18 M-29 Y), respectively, for surviving patients. The planned irradiation was completed in all patients. At the time of analysis in 2012, 8 patients were alive. Of the 8 patients who received PBT as initial treatment, 6 (75%) were alive with no evidence of disease, 1 was alive with distant metastasis, and 1 had died from tumor progression. Of the 6 patients who received PBT for recurrence, 1 was alive with no evidence of disease and 5 had died from tumor progression. The initial

Table 2 Clinical outcomes in 14 patients treated with proton beam therapy

Patient No	Cause of death	Survival after PBT (M)	Progression	Acute toxicity*	Late toxicity*
1	alive	349	none	none	vertebral growth retardation, narrowed aorta
2	alive	61	none	none	none
3	alive	40	none	none	none
4	alive	39	none	temporary hair loss, G1 pharyngitis	None
5	tumor	9	bone	G1 skin reaction	None
6	alive	20	none	None	G1 skin pigmentation
7	alive	20	bone marrow	None	none
8	alive	18	none	hair loss	thin hair
9	tumor	11	brain	G1 skin reaction	none
10	tumor	11	bone	none	none
11	tumor	31	bone marrow	none	none
12	tumor	27	lymph node	none	none
13	tumor	5	liver	none	-
14	alive	22	none	none	none

*G1: Grade 1 according to Criteria for Adverse Events version 3.0 of the National Cancer Institute and the late radiation morbidity scoring scheme of the Radiation Therapy Oncology Study Group/European Organization for Research and Treatment of Cancer.

progression sites were bone (n = 2), bone marrow (n = 2), liver (n = 1), brain (n = 1), and lymph nodes (n = 1).

Recurrence in the treatment field was not observed, but marginal failures occurred in 2 patients (Nos. 12, 13), resulting in a 3-year a locoregional control rate of 82% (CI: 59-100%) (Figure 1). One patient (No. 12) received PBT for a bulky recurrent tumor. This patient received PBT of 19.8 GyE for the pre-chemotherapy tumor volume, 30.6 GyE for the gross tumor volume, and 41.4 GyE for the gross tumor volume excluding the IORT field (Figure 2). The PTV margins were 5 mm because of the large irradiation volume. After completion of PBT, the tumor had disappeared, but paraaortic lymph node metastases appeared below the first irradiation field 17 months after PBT. This recurrent lesion was irradiated with about a 40% dose of 19.8 GyE. The second patient (No. 13) also received PBT for a bulky recurrent tumor invading the hepatic portal region (Figure 3). The irradiation field was too large to add the margin of 1.5 cm, and the whole tumor was included in the treatment field with a margin of 7 mm for the dose of 30.6 GyE, but the left kidney was blocked after 10.8 GyE. The tumor at the Morison fossa was excluded from the treatment field after 30.6 GyE by considering tolerance of the liver, and the treatment field was reduced to the main retroperitoneal tumor. The tumor shrunk in size, but disease progression occurred in the portal region beyond the irradiation field 5 months after PBT.

No severe acute toxicity was observed. A mild skin reaction and mucositis occurred in 3 patients and temporary hair loss in 2 as acute toxicity. Late toxicity was observed in 2 of the 13 patients who were followed up for more than 6 months. One of these patients was a neonatal case with stage 3 disease who reached adulthood. Retrospective measurement of the mitosis-karyorrhexis index (MKI) of pathological samples showed a favorable histology consistent with International Neuroblastoma Pathology Committee (INPC) criteria (low MKI and ≤1 year old at diagnosis). The MYCN status was not measured, but the patient may have been classified into the intermediate risk group with non-amplified MYCN, based on her survival. Thus, for a similar contemporary case, radiotherapy and chemotherapy would have been reduced; however, pathological and biological data for INRG risk grouping were not available in 1982 and she received PBT

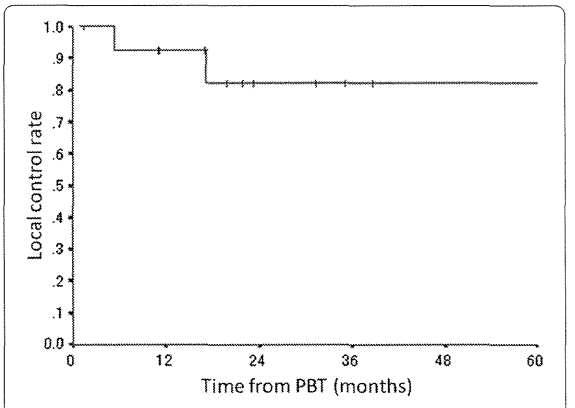

Figure 1 Local control rate for all patients.

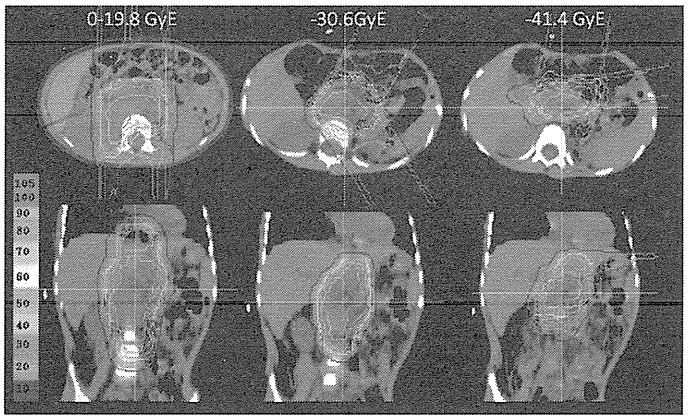

Figure 2 Dose distribution for patient No.12.

of 28.6 GyE in 13 fractions to the upper abdomen at age 1 year old. She visited our hospital due to unexplained occasional stomach pain during early pregnancy at 28 years after the PBT. The pain increased after eating, which caused loss of appetite. Thus, the patient did not gain enough weight during pregnancy and this resulted in a premature birth. A CT scan after birth showed vertebral growth retardation and a narrowed aorta, including the celiac artery (Figure 4). The reason for the stomach pain was concluded to be mesenteric ischemia due to stenosis of the superior mesenteric artery. Cilostazol was prescribed to increase blood flow and her stomach pain was relieved. There were no symptoms caused by vertebral growth retardation. The other patient received 19.8 GyE to the skull when he was 2 year old (Figure 5). Hair loss was prolonged, and his hair has been thin with some white hair from 18 months after PBT. No secondary cancer was observed.

Discussion

Recent progress of systemic therapies for advanced neuroblastoma has resulted in improved clinical outcomes, but local control is still an important concern. Panandiker et al. suggested that locoregional tumor control has an influence on overall survival [18], but gross resection is sometimes difficult because of bulky and invasive features involving critical organs. The prognosis of neuroblastoma with gross residual disease is poor and control is difficult, with Kushner et al. finding local recurrence in 3 of 7 patients with residual disease [3]. Neuroblastoma is highly sensitive to radiotherapy and a relatively low radiation dose of approximately 20 Gy is

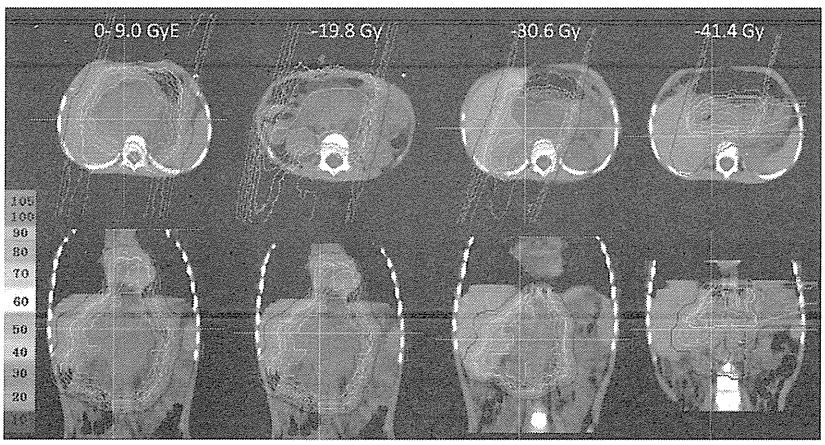

Figure 3 Dose distribution for patient No.13.

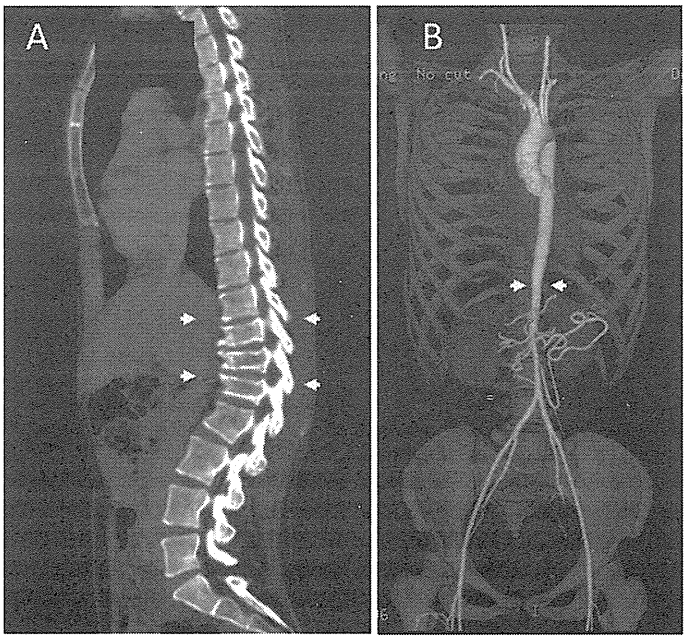

Figure 4 CT scan 28 years after the PBT. (**A**) Growth retardation in the ventral vertebral body. (**B**) Narrowing of the aorta below the irradiated field.

commonly used for minimal residual disease; however, the necessity for an escalated dose for gross residual disease has been suggested [19,20]. Kogan et al. reported an estimated 5-year locoregional recurrence rate of 51% for high risk primary neuroblastoma treated with 10 Gy for residual disease [19]. Compared with this, local recurrence was not observed in the patients with primary disease in our study, even though most patients had gross residual disease that was considered to be difficult to control by photon radiotherapy.

Recurrent neuroblastoma is also difficult to control, and sometimes acquires resistance to chemotherapy. Local radiotherapy for recurrent neuroblastoma has not been established. In our cases, most recurrent tumors were too large to be treated by photon radiotherapy, but around 20 Gy seemed to be insufficient for these tumors. Therefore, we treated 6 patients with recurrent disease using PBT with escalated doses from 30.6 to 45.5 GyE. Most of the patients eventually died, but 5 of the 6 had had an immediate complete response, with 2 surviving for more than 2 years after PBT and 1 patient still alive with no evidence of recurrence. These results suggest that PBT may contribute to improvement of the prognosis of patients with recurrent disease.

PBT is considered to be superior to intensity modulated radiation therapy (IMRT) for pediatric patients because higher doses can be delivered homogeneously to a large volume of neuroblastoma with a small number of ports while delivering very low doses in the path of the beam, which minimize the risk of a secondary cancer due to peripheral doses [10,12]. Hillbrand et al. suggested that PBT for pelvic neuroblastoma was preferred over IMRT because the dose distribution in IMRT produced a 1.5-fold greater risk of adverse events compared to PBT [10]. However, it is still important to monitor

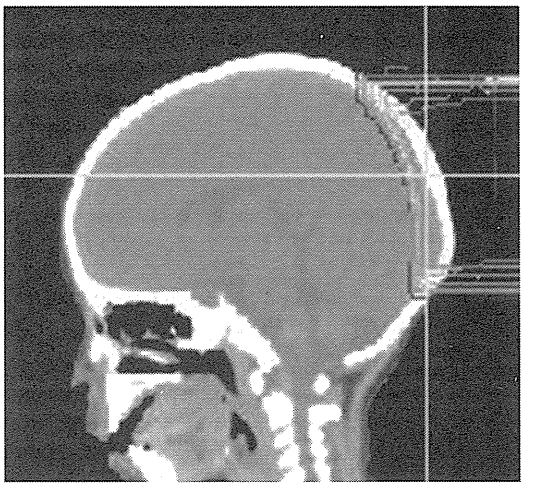

Figure 5 Proton irradiation of the skull reduces the dose to brain tissue.

possible toxicity after PBT and we experienced late toxicities in 2 patients. Follow-up is particularly important for girls for whom the aorta was included in the treatment field in PBT and photon radiotherapy because this may affect a future pregnancy. The threshold of aortic retardation is unclear; therefore, irradiation of the aorta should be avoided as much as possible by taking advantage of the proton dose distribution. Thus, the indication for PBT and photon radiotherapy in infancy should be carefully considered. Hair loss is generally only a minor problem after photon radiotherapy at 20 Gy, but this effect was prolonged in one of our patients. This may be because proton beams do not have a build-up effect and doses at the skin surface are higher than those in photon radiotherapy when the target is located near the surface. We choose proton as an alternative to electron beams to reduce cranial doses, but hair follicles are located 4 mm deep in the skin and the lethal dose for hair follicles is 16 Gy [21]. This indicates that the treatment field and indication should be carefully determined to optimize the utilization of the characteristics of proton beams.

Until recently, PBT was viewed as a novel therapy, and therefore we had mainly used PBT to treat patients with neuroblastoma that was difficult to manage, with most of these patients having gross residual disease. Management with photon radiotherapy was difficult in 8 of the 14 patients in the study and PBT was chosen as a potential treatment option. The outcomes in these cases were favorable and little severe toxicity occurred, even though higher doses (> 20 Gy) were used for some patients. Our study is limited by the small number of patients and restriction of long-term follow-up to only one patient, but the results suggested that PBT may be conducted safely for patients with neuroblastoma that is difficult to manage using photon beams.

Conclusions

PBT may be conducted safely for patients with neuroblastoma that is difficult to manage using photon beams.

Abbreviations

PBT: Proton beam therapy; INSS: International Neuroblastoma Staging System; INRG: The international neuroblastoma risk group; IORT: Intraoperative radiotherapy; CTV: Clinical target volume; PTV: Planning target volume; MKI: Mitosis-karyorrhexis index; INPC: International Neuroblastoma Pathology Committee; IMRT: Intensity modulated radiation therapy.

Competing interests

The authors declared that they have no competing interests.

Authors' contributions

YO selected the data and performed the analysis, drafted and wrote the manuscript. TF and TN planned and conducted chemotherapy. HO and MK performed surgery and chemotherapy. YO, MM, TO, SS, HI, TH, KT, and HS conducted radiotherapy. YO, TO, TF, MK, and HS reviewed/ revised the article. All authors read and approved final manuscript.

Acknowledgment

This work was supported by the "Funding Program for World-Leading Innovative R&D on Science and Technology (FIRST Program)", initiated by the Council for Science and Technology Policy (CSTP).

Author details

[1]Department of Radiation Oncology, University of Tsukuba, Tennodai 1-1-1, Tsukuba, Ibaraki, Japan. [2]Department of Pediatrics, University of Tsukuba, Ibaraki, Japan. [3]Department of Pediatric Surgery, University of Tsukuba, Ibaraki, Japan. [4]Department of Radiation Oncology, Tokyo Medical University Ibaraki Medical Center, Ami, Inashiki, Ibaraki, Japan.

Received: 18 January 2013 Accepted: 1 June 2013
Published: 12 June 2013

References

1. Berthold F, Boos J, Burdach S, Erttmann R, Henze G, Hermann J, Klingebiel T, Kremens B, Schilling FH, Schrappe M, *et al*: **Myeloablative megatherapy with autologous stem-cell rescue versus oral maintenance chemotherapy as consolidation treatment in patients with high-risk neuroblastoma: a randomised controlled trial.** *Lancet Oncol* 2005, **6**:649–658.
2. Kaneko M, Tsuchida Y, Mugishima H, Ohnuma N, Yamamoto K, Kawa K, Iwafuchi M, Sawada T, Suita S: **Intensified chemotherapy increases the survival rates in patients with stage 4 neuroblastoma with MYCN amplification.** *J Pediatr Hematol Oncol* 2002, **24**:613–621.
3. Kushner BH, Wolden S, LaQuaglia MP, Kramer K, Verbel D, Heller G, Cheung NK: **Hyperfractionated low-dose radiotherapy for high-risk neuroblastoma after intensive chemotherapy and surgery.** *J Clin Oncol* 2001, **19**:2821–2828.
4. Matthay KK, Villablanca JG, Seeger RC, Stram DO, Harris RE, Ramsay NK, Swift P, Shimada H, Black CT, Brodeur GM, *et al*: **Treatment of high-risk neuroblastoma with intensive chemotherapy, radiotherapy, autologous bone marrow transplantation, and 13-cis-retinoic acid. Children's Cancer Group.** *N Engl J Med* 1999, **341**:1165–1173.
5. La Quaglia MP, Kushner BH, Heller G, Bonilla MA, Lindsley KL, Cheung NK: **Stage 4 neuroblastoma diagnosed at more than 1 year of age: gross total resection and clinical outcome.** *J Pediatr Surg* 1994, **29**:1162–1165. discussion 1165–1166.
6. Simon T, Berthold F, Borkhardt A, Kremens B, De Carolis B, Hero B: **Treatment and outcomes of patients with relapsed, high-risk neuroblastoma: results of German trials.** *Pediatr Blood Cancer* 2011, **56**:578–583.
7. Garaventa A, Parodi S, De Bernardi B, Dau D, Manzitti C, Conte M, Casale F, Viscardi E, Bianchi M, D'Angelo P, *et al*: **Outcome of children with neuroblastoma after progression or relapse. A retrospective study of the Italian neuroblastoma registry.** *Eur J Cancer* 2009, **45**:2835–2842.
8. Rich BS, McEvoy MP, LaQuaglia MP, Wolden SL: **Local control, survival, and operative morbidity and mortality after re-resection, and intraoperative radiation therapy for recurrent or persistent primary high-risk neuroblastoma.** *J Pediatr Surg* 2011, **46**:97–102.
9. Athar BS, Paganetti H: **Comparison of second cancer risk due to out-of -field doses from 6-MV IMRT and proton therapy based on 6 pediatric patient treatment plans.** *Radiother Oncol* 2011, **98**:87–92.
10. Hillbrand M, Georg D, Gadner H, Potter R, Dieckmann K: **Abdominal cancer during early childhood: a dosimetric comparison of proton beams to standard and advanced photon radiotherapy.** *Radiother Oncol* 2008, **89**:141–149.
11. Kozak KR, Adams J, Krejcarek SJ, Tarbell NJ, Yock TI: **A dosimetric comparison of proton and intensity-modulated photon radiotherapy for pediatric parameningeal rhabdomyosarcomas.** *Int J Radiat Oncol Biol Phys* 2009, **74**:179–186.
12. Heinzelmann F, Thorwarth D, Lamprecht U, Kaulich TW, Fuchs J, Seitz G, Ebinger M, Handgretinger R, Bamberg M, Weinmann M: **Comparison of different adjuvant radiotherapy approaches in childhood bladder/ prostate rhabdomyosarcoma treated with conservative surgery.** *Strahlenther Onkol* 2011, **187**:715–721.
13. Lorentini S, Amichetti M, Spiazzi L, Tonoli S, Magrini SM, Fellin F, Schwarz M: **Adjuvant intensity-modulated proton therapy in malignant pleural mesothelioma. A comparison with intensity-modulated radiotherapy and a spot size variation assessment.** *Strahlenther Onkol* 2012, **188**:216–225.

14. Hattangadi JA, Rombi B, Yock TI, Broussard G, Friedmann AM, Huang M, Chen YL, Lu HM, Kooy H, Macdonald SM: **Proton radiotherapy for high-risk pediatric neuroblastoma: early outcomes and dose comparison.** *Int J Radiat Oncol Biol Phys* 2012, **83**:1015–1022.
15. Monclair T, Brodeur GM, Ambros PF, Brisse HJ, Cecchetto G, Holmes K, Kaneko M, London WB, Matthay KK, Nuchtern JG, *et al*: **The International Neuroblastoma Risk Group (INRG) staging system: an INRG Task Force report.** *J Clin Oncol* 2009, **27**:298–303.
16. Tsunashima Y, Sakae T, Shioyama Y, Kagei K, Terunuma T, Nohtomi A, Akine Y: **Correlation between the respiratory waveform measured using a respiratory sensor and 3D tumor motion in gated radiotherapy.** *Int J Radiat Oncol Biol Phys* 2004, **60**:951–958.
17. Oshiro Y, Okumura T, Ishida M, Sugahara S, Mizumoto M, Hashimoto T, Yasuoka K, Tsuboi K, Sakae T, Sakurai H: **Displacement of hepatic tumor at time to exposure in end-expiratory-triggered-pulse proton therapy.** *Radiother Oncol* 2011, **99**:124–130.
18. Pai Panandiker AS, McGregor L, Krasin MJ, Wu S, Xiong X, Merchant TE: **Locoregional tumor progression after radiation therapy influences overall survival in pediatric patients with neuroblastoma.** *Int J Radiat Oncol Biol Phys* 2010, **76**:1161–1165.
19. Haas-Kogan DA, Swift PS, Selch M, Haase GM, Seeger RC, Gerbing RB, Stram DO, Matthay KK: **Impact of radiotherapy for high-risk neuroblastoma: a Children's Cancer Group study.** *Int J Radiat Oncol Biol Phys* 2003, **56**:28–39.
20. Kremens B, Klingebiel T, Herrmann F, Bender-Gotze C, Burdach S, Ebell W, Friedrich W, Koscielniak E, Schmid H, Siegert W, *et al*: **High-dose consolidation with local radiation and bone marrow rescue in patients with advanced neuroblastoma.** *Med Pediatr Oncol* 1994, **23**:470–475.
21. Severs GA, Griffin T, Werner-Wasik M: **Cicatricial alopecia secondary to radiation therapy: case report and review of the literature.** *Cutis* 2008, **81**:147–153.

doi:10.1186/1748-717X-8-142
Cite this article as: Oshiro *et al.*: Clinical results of proton beam therapy for advanced neuroblastoma. *Radiation Oncology* 2013 **8**:142.

Int J Clin Oncol (2013) 18:389–395
DOI 10.1007/s10147-012-0391-y

ORIGINAL ARTICLE

Successful treatment of infants with localized neuroblastoma based on their *MYCN* status

Tomoko Iehara · Minoru Hamazaki · Tatsuro Tajiri · Yoshifumi Kawano · Michio Kaneko · Hitoshi Ikeda · Hajime Hosoi · Tohru Sugimoto · Tadashi Sawada · Japanese Infantile Neuroblastoma Cooperative Study Group

Received: 10 September 2011 / Accepted: 12 February 2012 / Published online: 2 March 2012

Abstract
Background The aim of this study was to evaluate the effectiveness of post-surgical chemotherapy for infants with localized neuroblastoma without *MYCN* amplification (MNA), and determine whether risk classification using MNA is reasonable.
Methods Four hundred and fourteen eligible patients were registered between 1998 and 2004. Resectable patients in stage 1 and 2A/2B were treated by surgical resection only. Unresectable patients in stage 3 without MNA received either 6 cycles of regimen A or 3 cycles of regimen A plus 3 cycles of regimen C2; regimen A consisted of low doses of cyclophosphamide and vincristine and regimen C consisted of cyclophosphamide, vincristine and pirarubicin before surgical resection. The resectable and unresectable patients were randomly selected to receive post-surgical chemotherapy. The patients with MNA received intensive chemotherapy regimen D2, consisting of cyclophosphamide, vincristine, pirarubicin and cisplatin, and some of them received high-dose chemotherapy with stem cell transplantation.
Results The 5-year event-free survival (5-EFS) rates of stage 1 and 2A/2B patients without MNA were 97.2 and 89.0% respectively ($p = 0.02$). A total of 31 patients in stage 3 without MNA received post-surgical chemotherapy, and 30 patients did not. The 5-EFS rates of these two groups (96.0 and 96.2%, respectively) were not significantly different ($p = 0.869$). The 5-EFS rate for localized patients with MNA ($n = 6$) was 50.0%, and that of patients without MNA was 95.0% ($p < 0.001$).
Conclusion Post-surgical chemotherapy was therefore unnecessary for localized patients without MNA. This treatment strategy using MNA is considered to be appropriate in infants.

Keywords Localized neuroblastoma · Infants · Chemotherapy · *MYCN* amplification

T. Iehara (✉) · H. Hosoi · T. Sugimoto · T. Sawada
Department of Pediatrics, Graduate School of Medical Science, Kyoto Prefectural University of Medicine, Kawaramachi-Hirokoji, Kamigyo-ku, Kyoto 602-8566, Japan
e-mail: iehara@koto.kpu-m.ac.jp

M. Hamazaki
Department of Pathology, Shizuoka Children's Hospital, Shizuoka 420-8660, Japan

T. Tajiri
Department of Pediatric Surgery, Graduate School of Medical Sciences, Kyushu University, Fukuoka 812-8582, Japan

Y. Kawano
Department of Pediatrics, Kagoshima University Graduate School of Medical and Dental Sciences, Kagoshima 890–8520, Japan

M. Kaneko
Department of Pediatric Surgery, Institute of Clinical Medicine, Graduate School of Comprehensive Human Sciences, University of Tsukuba, Tsukuba, Ibaraki 305-8575, Japan

H. Ikeda
Department of Pediatric Surgery, Dokkyo Medical University Koshigaya Hospital, Koshigaya, Saitama 343-8555, Japan

Introduction

The prognosis of neuroblastoma patients improves with decreasing age, and the prognosis of infantile patients is especially good. A nationwide mass screening program for 6-month-old infants was initiated in Japan in 1985 for the early detection of neuroblastoma [1, 2], and resulted in an increased detection of early-stage infantile neuroblastoma.

The prognoses of the patients detected in the mass screening, most of whom were infantile neuroblastoma patients, were excellent [3]. Many patients of early-stage localized neuroblastoma were found to have been unnecessarily treated with chemotherapy after surgical resection [4]. Chemotherapy was also reduced in Italy [5]. However, excessive chemotherapy was still being ordered for many localized neuroblastoma cases in infants, even though physicians in Japan in the early 1990s realized that less treatment was needed. On the other hand, *MYCN* amplification (MNA) is the most powerful prognostic factor, but there is no consensus as to whether low-stage patients with MNA should be classified a high risk. The Japanese Infantile Neuroblastoma Cooperative Study Group classifies infants with neuroblastoma using MNA and stage and assigns treatments.

The first prospective study (#9405) to examine the effectiveness of post-surgical chemotherapy for cases of stage 1 and 2 localized tumors in infants with neuroblastoma based on *MYCN* status was started in June 1994 [6]. A second study (#9805) that examined the effectiveness of post-surgical chemotherapy in localized stage 3 tumors without MNA was initiated in June 1998, and was concluded in December 2004. This paper reports on the results of this study, and discusses the effectiveness of postsurgical chemotherapy for localized neuroblastoma cases in infants.

A	Vincristine	1.5mg/m^2	day1	
	Cyclophosphamide	300mg/m^2	day8	/2W
C2	Vincristine	1.5mg/m^2	day1	
	Cyclophosphamide	600mg/m^2	day1	
	Pirarubicin	30mg/m^2	day3	/4W
D2	Vincristine	1.5mg/m^2	day1	
	Cyclophosphamide	900mg/m^2	day1	
	Pirarubicin	30mg/m^2	day3	
	Cisplatin	12mg/m^2	day1-5	/4W

Fig. 1 Chemotherapy regimens for patients with infantile neuroblastoma. Babies less than 6 months old were treated with reduced dosages: 1/3 dose for infants of less than 2 months, 1/2 dose for infants of 2–4 months, and 2/3 dose for infants ranging from 4 to 6 months of age

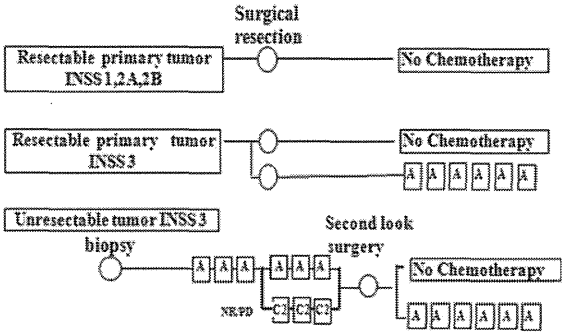

Fig. 2 Study #9805 for *MYCN* non-amplified neuroblastoma patients in stages 1, 2A, 2B and 3. Details of regimens are given in "Patients and methods". After surgical resection, stage 3 patients were randomly assigned to either receive post-surgical chemotherapy (6 cycles of regimen A) or not. *NR* no response, *PD* progressive disease

Patients and methods

Four hundred and twenty-nine patients were registered with study #9805 between June 1998 and December 2004, and 414 patients were eligible to be included in the study based on criteria. The age at diagnosis was between 0 and 14 months, and the median age was 7.35 months. Disease extension was evaluated according to the International Neuroblastoma Staging System (INSS) [7]. Histological investigation of the primary tumor was mandatory to allow diagnosis of the neuroblastoma according to the International Neuroblastoma Pathology Classification, with the central review system by the Committee of Japanese Pediatric Tumor Pathology [8]. MNA of tumor samples were detected by either a FISH (fluorescence in-situ hybridization) analysis or a Southern blot analysis, according to standard procedures [9]. Patients with 10 copies or more of the *MYCN* gene were considered to have MNA.

Treatment

Three chemotherapy regimens were used in this study, regimens A, C2, and D2 (Fig. 1). One cycle of regimen A comprised a low dose of cyclophosphamide (CPM 300 mg/m^2) on day 1 and a dose of vincristine (VCR 1.5 mg/m^2) on day 8 over a 2-week period. One cycle of regimen C2 comprised 600 mg/m^2 CPM and 1.5 mg/m^2 VCR on day 1 and 30 mg/m^2 pirarubicin (THP-ADR) on day 3 over a 4-week period. Regimen D2 comprised 900 mg/m^2 CPM and 1.5 mg/m^2 VCR on day 1 and 30 mg/m^2 THP-ADR on day 3 and cisplatin (CDDP) 12 mg/m^2 from day 1 to day 5 over a 4-week period.

The patients in stages 1, 2A and 2B without MNA were treated by surgical resection only. The resectable patients in stage 3 without MNA were randomly assigned to either receive post-surgical chemotherapy (6 cycles of regimen A) or not receive further therapy after surgical resection (Fig. 2). Unresectable patients were given either 6 cycles of regimen A or 3 cycles of regimen A followed by 3 cycles of regimen C2 to shrink the tumor, followed by